Nonlinear Dyn (2022) 108:765–787
https://doi.org/10.1007/s11071-022-07199-8

ORIGINAL PAPER

Nonlinear wave propagation in locally dissipative metamaterials via Hamiltonian perturbation approach

Alessandro Fortunati · Andrea Bacigalupo · Marco Lepidi · Andrea Arena · Walter Lacarbonara

Received: 2 August 2021 / Accepted: 30 November 2021 / Published online: 2 February 2022

Abstract The cellular microstructure of periodic architected materials can be enriched by local intracellular mechanisms providing innovative distributed functionalities. Specifically, high-performing mechanical metamaterials can be realized by coupling the low-dissipative cellular microstructure with a periodic distribution of tunable damped oscillators, or resonators, vibrating at relatively high amplitudes. The benefit is the actual possibility of combining the design of wave-stopping bands with enhanced energy dissipation properties. This paper investigates the nonlinear dispersion properties of an archetypal mechanical metamaterial, represented by a one-dimensional lattice model characterized by a diatomic periodic cell. The intracellular interatomic interactions feature geometric and constitutive nonlinearities, which determine cubic coupling between the lattice and the resonators. The non-dissipative part of the coupling can be designed to exhibit a softening or a hardening behavior, by independently tuning the geometric and elastic stiffnesses. The nonlinear wavefrequencies and waveforms away from internal resonances are analytically determined by adopting a perturbation technique. The employed approach makes use of tools borrowed from Hamiltonian perturbation theory, together with techniques often used in the context of nearly-integrable Hamiltonian systems.The dispersion spectra are determined in closed, asymptotically approximate, form as a nonlinear function of the time-dependent decreasing amplitude decrement. The invariant manifolds defined by the harmonic periodic motions are also analytically determined. The asymptotic results are further validated numerically.

Keywords Mechanical metamaterials · Nonlinear wave propagation · Vibration absorbers · Cubic nonlinearities · Energy dissipation · Asymptotic techniques · Lie series

A. Fortunati (✉)· A. Arena · W. Lacarbonara
DISG - Sapienza University of Rome, Rome, Italy
e-mail: alessandro.fortunati@uniroma1.it

A. Arena
e-mail: andrea.arena@uniroma1.it

W. Lacarbonara
e-mail: walter.lacarbonara@uniroma1.it

A. Bacigalupo · M. Lepidi
DICCA - University of Genoa, Genoa, Italy
e-mail: andrea.bacigalupo@unige.it

M. Lepidi
e-mail: marco.lepidi@unige.it

1 Introduction

Future aerostructures performance will be enhanced by advances in lightweight, strong, highly damped multifunctional composites [1–6]. In parallel with the development of new polymeric composites with high strength-to-mass ratios, the demand of damping capacity will be increasing to ensure safe operations across adverse dynamic conditions. Conventional approaches based on viscoelastic or elastomeric constrained damp-

ing tend to be not effective due to poor thermal properties and stiffness/strength mismatch with the hosting matrix. New highly damping nanocomposite materials with carbonaceous nanofillers have been proposed to exploit nanoscale effects such as those associated with sliding crystals on nanofillers acting as distributed nanopistons [7,8].

Alternative to multi-phase material approaches, innovative materials possessing periodic cellular structures are being explored in the literature [9–11] with the objective of tailoring the dynamic properties of the unit cells toward increased vibration absorption properties or the creation of bandgaps which can stop the propagation of waves across targeted frequency bands and wavelengths. These materials, also known as mechanical metamaterials, are macro/micro-architected media characterized by non-conventional features and designed for advanced applications such as passive attenuation of elastic waves [12], broadband sound absorption and low-frequency noise filtering [13–17] or other unusual dynamic properties [18,19]. The growing success of mechanical metamaterials is also sustained by the recent extraordinary developments in the technical and technological fields of high-fidelity computational mechanics, micro-engineering design and high-precision additive manufacturing [20].

Unlike phononic crystals, mechanical (or acoustic) metamaterials can be also engineered at the micro structural level so as to achieve optimal dispersion properties by designing cells configurations including local resonators and exploiting the dynamic features arising from the modal interaction and enhanced by the periodicity of the micro structure [21–23]. Densely distributed resonators can be introduced in metamaterials to obtain band gaps and avoid wave propagation in the neighborhood of selected resonance frequencies through the mechanism of energy transfer between the periodic structure and the local resonators [24–26].

This is a radically different approach with respect to conventional absorbers architectures making use of one or a few macroscopic (large in scale) vibration absorbers [27,28]. Cellular material concepts with embedded periodic devices aim to strategically spread out the multitude of absorbers in the unit cells within the hosting structure. In [29] a beam embedding a periodic array of nonlinear absorbers was shown to possess much wider vibration suppression bandwidth. The mass distribution allows an overall weight reduction of the damping system not only because of its colloca-

tion in dedicated hotspots, but also because the much smaller masses can be supported by significantly lighter structures.

In [30], a novel architected lattice metamaterial with broadband and multiband bandgap characteristics was studied showing that a slight structural modification in a regular lattice structure resulted in augmented vibration attenuation capability. The insertion of circular masses at the center of these lattices helped induce multiband low frequency bandgaps. In [31], a locally resonant elastic metamaterial based on liquid solid interaction was proposed to attenuate flexural wave propagation across a broad low frequency range. To provide the capability of filtering at the ultra-low frequency and, at the same time, to ensure the lowest weight of the structure, the topological and mechanical optimization of acoustic metamaterials embedding local resonators necessarily implies that the latter must possess a very low stiffness together and a very small mass [32–35]. Moreover, since these resonators are characterized by low dissipation properties, high-amplitude oscillations are necessary to deliver an efficient energy transfer between the periodic micro-structure and the resonators, thus implying a non-negligible role of the geometric nonlinearities [36–38]. In [39] a historical overview of metamaterials is provided, first addressing their interesting linear properties, and, then, showing how these give rise to exotic nonlinear properties.

This topic has attracted the interest of nonlinear dynamicists for years. Several authors, for example, adopted asymptotic approaches, such as the method of multiple scales [40], to investigate the nonlinear resonance scenarios in periodic structures. This approach leads to closed-form expressions of the bifurcations and sensitivity analyze. In [41] a multiple-scale approach was presented to capture internally resonant wave interactions in weakly nonlinear lattices and metamaterials, while in [42] this method was employed to study analytically the dispersion properties characterizing the free propagation of harmonic waves in pantographic metamaterials. The standing and traveling waves in undamped periodic systems possessing cubic nonlinearities were studied asymptotically both with or without 3:1 internal resonances in [43,44] and, more recently, in [45] where it was shown that the method of multiple scales provides more general results than Lindstedt-Poincaré in the case of wave-wave interactions. Other, interesting, examples of the use of the method of multiple scales can be found in [46] where

the effect of nonlinear hyperelastic interactions was investigated between a rubberlike elastomeric local resonator and the hosting matrix showing new dynamic phenomena such as the appearance of half subharmonic attenuation zones complementing the local resonance band gap around the fundamental frequency. Recently, the method of multiple scales has been employed in combination with a standard continualization scheme (see for details [47–49]) to study the effects of nonlinear wave modulations on the band structure of a one-dimensional acoustic metamaterial characterized by linearly damped local resonators [50]. An asymptotic approach was also adopted in [51] to study the formation of discrete traveling breathers in a 1D semi-infinite, linearly grounded, essentially nonlinear lattice, generated by an impulsive excitation. The existence of a nonlinear propagation zone and two attenuation zones was proven in the acoustics of the corresponding infinite lattice. Further studies [52] made use of nonlinear maps to investigate the propagation properties of waves in one-dimensional chains of coupled nonlinear oscillators. Finally, the harmonic balance method, properly modified according to a asymptotic ordering of the harmonic amplitudes, was adopted in [53] to study the influence of the nonlinearities on the filtering properties in one-dimensional chains with attached nonlinear local oscillators.

In [54], a high-order spatio-temporal gradient expansion was used to localize the multiscale problem leading to a series of recursive unit cell problems providing the appropriate micro-mechanical corrections. More recently, the amplitude-dependent band structure of weakly nonlinear lattices with monoatomic and diatomic periodic cells was investigated asymptotically and numerically [55,56]. Similar periodic systems, although featuring strong nonlinearities, were studied via the semi-analytical series expansion method [57, 58]. The nonlinear dynamic interactions between two internally resonant waves were addressed when these waves travel through an undamped monoatomic chain of point masses interconnected by linear and cubic springs. Some of these nonlinear phenomena were also experimentally investigated. An experimental proof of a sub-harmonic transmission attenuation zone due to energy exchange induced by autoparametric resonance in locally resonant metamaterials was presented.

In parallel to asymptotic techniques applied directly to the ODEs or PDEs governing the wave propagation problem, other works [59] and [60] showed how asymptotic results involving systems of ODEs close to integrability (either autonomous or non-autonomous) can be obtained by using the extensively developed tools of Hamiltonian Perturbation Theory. The key step consists in the definition of an equivalent Hamiltonian system in a suitably *extended phase space*. Along these lines, in this paper a perturbation analysis of a nonlinear system of ODEs is carried out in the neighborhood of a "close-to-elliptic" hyperbolic equilibrium. Investigating the dynamics of nearly-integrable Hamiltonian systems is a problem enjoying a long and well established tradition, dating back to Poincaré [61]. Since then, the field of dynamic systems has witnessed an intense development of perturbation tools in order to study and generalize this problem, with the ultimate goal of tackling the challenging *small divisors problem* [62–64]. In this respect, the milestone contributions about the stability issues obtained by Nekhoroshev [65], [66] and by Kolmogorov, Arnol'd and Moser (commonly known as KAM Theorem [67]) are worth to be mentioned.

Perturbation approaches, based on the so-called *Lie series* and *Lie transform* [68], have been profitably exploited in various applications for a key feature, namely, these methods do not require any inversion of the variable transformations. This has had remarkable consequences for their automatic implementations, as strategically done in this paper. More details about the mentioned methods can be found, for instance, in [69] and [70]. Another remarkable advantage of the Hamiltonian formulation is that the problem can be studied up to an arbitrary high order of normalization by using constructive and explicit algorithms such as the mentioned Lie Transform method. It is interesting to point out that either the Lie series or the Lie transform method, in the formalism developed by Giorgilli [70], turned out to be successful in the generalization to the case of nearly integrable non autonomous systems with a general (i.e., *aperiodic*) time dependence [59,71–73].

2 A one-dimensional dissipative metamaterial

2.1 Nonlinear equations of motion of the periodic cell

The minimal physical archetype of a mechanical metamaterial can be realized by an infinite one-dimensional periodic chain of stiff rings, each hosting a tunable *local resonator* characterized by geometric and constitutive nonlinearities and playing the role of vibration

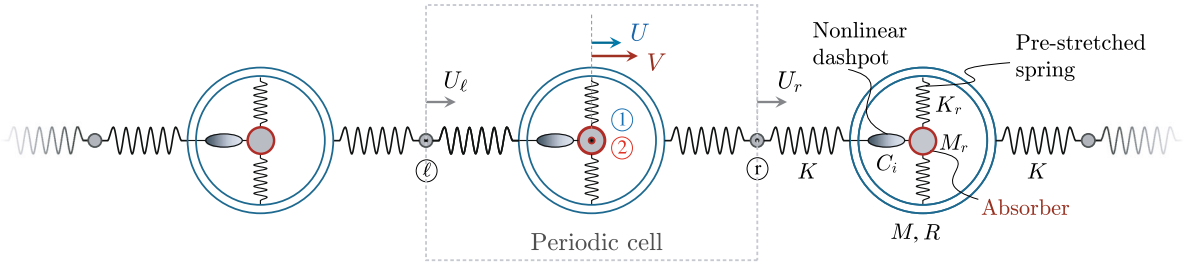

Fig. 1 Minimal acoustic metamaterial realized by a one-dimensional lattice featuring a diatomic periodic cell with intra-cellular nonlinear vibration absorbers

absorber (Fig. 1). The dynamic behavior of the metamaterial microstructure can be governed by a synthetic discrete lattice model. The stiff ring of the periodic cell can be modeled as perfectly rigid with mean radius R and translational mass M, exchanging purely attractive or repulsive conservative forces with the adjacent rings of the chain. Considering the static equilibrium as the reference configuration, the current configuration of the ring is described by the chain-aligned displacement $U(t)$ of the microstructural node ① located at the ring center of mass. The vibration absorber can be modeled as a point mass M_r, exchanging only intra-cellular forces with the hosting ring. The current configuration of the absorber is described by the chain-aligned displacement $V(t)$ of the microstructural node ②. Accordingly, the positions of the configurational nodes ① and ② are the same in the reference configuration.

The inter-cellular interactions (short-range forces) are described by linear elastic springs (*primary springs*) with spring stiffness K, connecting the rigid ring with the auxiliary massless nodes ⓡ and ⓛ located at the cell boundaries. Accordingly, the external forces exerted on the reference cell by the adjacent cells read

$$\begin{aligned} N_r(U, U_r) &= K(U_r - U), \\ N_\ell(U, U_\ell) &= K(U_\ell - U), \end{aligned} \tag{1}$$

where U_r and U_ℓ are the chain-aligned displacements of the nodes ⓡ and ⓛ, respectively.

The intra-cellular *non dissipative* interaction between the ring and the absorber can be described by a pair of prestressed springs orthogonal to the chain (*secondary springs*), determining a conservative force proportional to the relative displacement $W(t) = V(t) - U(t)$ according to the geometrically exact formula

$$F_N(W) = 2K_r W + 2(N_0 - K_r R)\frac{W}{\sqrt{R^2 + W^2}} \tag{2}$$

where K_r and N_0 are the linear elastic stiffness and pretension ($N_0 > 0$) of the secondary springs, respectively.

The intra-cellular *dissipative* interaction between the ring and the absorber can be described instead by a chain-aligned nonlinear daashpot whose constitutive law was first proposed in [74], exhibiting a non-conservative force proportional to the relative velocity $\dot{W}(t) = \dot{V}(t) - \dot{U}(t)$ according to the formula

$$N_{dr}(W, \dot{W}) = C_1\left(1 - C_2 \exp(-C_3 W^2)\right)\dot{W}, \tag{3}$$

where the overdot indicates differentiation with respect to time t. The coefficients C_1 and C_2 regulate the linear and nonlinear contributions to the viscous damping. Phenomenologically, the sign of C_2 governs the rate of energy dissipation and a positive value produces pinching in the resulting hysteresis cycle, thus reducing the rate of dissipation at low displacement amplitudes. Coefficient C_3 regulates the pinching extension about the origin of the hysteresis cycles.

By considering a characteristic length L of the periodic cell (a convenient choice is $L = R$), nondimensional variables are introduced in the form

$$\tau = \Omega t, \quad u = \frac{U}{L}, \quad w = \frac{W}{L}, \quad u_r = \frac{U_r}{L}, \quad u_\ell = \frac{U_\ell}{L} \tag{4}$$

where $\Omega^2 = K/M$ is the (squared) characteristic frequency of the undamped oscillator with mass M and

spring constant K. A minimal set of independent nondimensional parameters is

$$\begin{aligned} \varrho^2 &= M_r/M, \quad & \xi_1 &= C_1\Omega L/(RK), \\ \mu &= N_0/(KL), & \xi_2 &= C_2, \\ \eta &= K_r/K, & \xi_3 &= C_3 L^2, \end{aligned} \tag{5}$$

where ϱ^2 is the mass ratio between the absorber and the ring ($\varrho \neq 0$), while μ and η describe the nondimensional geometric and elastic stiffnesses of the secondary springs ($\mu > 0$, $\eta > 0$), and ξ_1, ξ_2, ξ_3 are the nondimensional coefficients regulating the nonlinear viscosity of the dashpots ($\xi_1 \geq 0$, $-1 < \xi_2 < 1$, $\xi_3 > 0$). From a physical viewpoint, *heavy* highly-massive and low-deformable metamaterials (with small ϱ^2 and η) can be conventionally distinguished from *light* low-massive and high-deformable metamaterials (with large ϱ^2 and η), for certain fixed resonator properties K_r and M_r.

The nondimensional form of the nonlinear ordinary differential equations of motion governing the free damped dynamics of the periodic cell is obtained as

$$\begin{aligned} &(1+\varrho^2)\ddot{u} + \varrho^2\ddot{w} + 2u - u_r - u_\ell = 0, \\ &\varrho^2\ddot{u} + \varrho^2\ddot{w} + G(w, \dot{w}; \boldsymbol{\xi}) + F(w; \mu, \eta) = 0, \end{aligned} \tag{6}$$

where the overdot now indicates differentiation with respect to the nondimensional time τ. The *active* degrees of freedom u and w can be distinguished from the *passive* degrees of freedom u_r and u_ℓ. Both passive degrees of freedom are quasi-statically coupled with the active degree of freedom u through the nondimensional linear inter-cellular constitutive relations $n_\ell = u_\ell - u$ and $n_r = u_r - u$, where $n_\ell = N_\ell/(KL)$ and $n_r = N_r/(KL)$ are the nondimensional passive forces. The nondimensional intra-cellular forces characterizing the ring-resonator coupling features two contributions

$$\begin{aligned} G(w; \dot{w}, \boldsymbol{\xi}) &:= \xi_1 \dot{w} \left(1 - \xi_2 \exp(-\xi_3 w^2)\right), \\ F(w; \mu, \eta) &:= 2w \left(\eta + (\mu - \eta)/\sqrt{1 + w^2}\right) \end{aligned} \tag{7}$$

where $\boldsymbol{\xi} := (\xi_1, \xi_2, \xi_3)$ is the vector collecting the viscosity coefficients.

By considering the total viscoelastic restoring force $\mathfrak{G}(w, \dot{w}) = F(w; \mu, \eta) + G(w; \dot{w}, \boldsymbol{\xi})$, a family of hysteresis loops corresponding to a prescribed time-periodic displacement $w(\tau) = w_0 \sin\tau$ in the $(\mathfrak{G}, w)$-plane is shown in Fig. 2. From a qualitative viewpoint, this model enables the possibility of tailoring the constitutive behavior of the ring-resonator coupling to achieve a softening or hardening response for a given geometric stiffness ($\mu = 1/2$), by properly reducing ($\eta = 5/100$ so that $\mu - \eta < 0$, see Fig. 2a,b,c) or increasing ($\eta = 125/100$ so that $\mu - \eta > 0$, see Fig. 2d,e,f) the elastic spring constant ratio. From a quantitative viewpoint, the dissipated energy increases for larger values of the parameter ξ_1, while the purely elastic backbone behavior corresponding to the nonlinear force-displacement curve is recovered for $\xi_1 = 0$ (Fig. 2a,d). The pinching effect on the hysteresis loops caused by increasing values of the parameter ξ_2 can also be noticed (Fig. 2b,e). The hysteresis loops corresponding to different amplitudes are proven to lie on the surfaces defined by the softening or hardening restoring force $\mathfrak{G}(w, \dot{w})$ over the $(w, \dot{w})$-plane (Fig. 2c,f).

2.2 Wave propagation

The free propagation of elastic waves through the dissipative mechanical metamaterial can be analyzed by means of the Floquet-Bloch theory for periodic structures [75]. This theory is applicable to periodic systems with linear intercellular coupling forces in the framework of perturbation methods [22,37]. Specifically, a family of harmonic wave solutions can be obtained by enforcing quasi-periodicity between the dynamic variables (displacements and forces) at the opposite edges of the cell boundary

$$u_r = u_\ell \exp(-\imath\beta), \qquad n_r = -n_\ell \exp(-\imath\beta), \tag{8}$$

where β is the nondimensional wavenumber, spanning the one-dimensional Brillouin zone $\mathcal{B} = (-\pi, \pi)$. Therefore, the passive degrees of freedom can be condensed as quasi-static functions of the active degrees of freedom, according to the relations

$$\begin{aligned} u_\ell &= \tfrac{1}{2}(1 + \exp(i\beta))u, \\ n_\ell &= \tfrac{1}{2}(1 - \exp(i\beta))u \end{aligned} \tag{9}$$

where the quasi-periodicity conditions (8) have been employed. Consequently, the nonlinear equations of motion can be reformulated in the reduced space spanning the active degrees of freedom only. Accordingly,

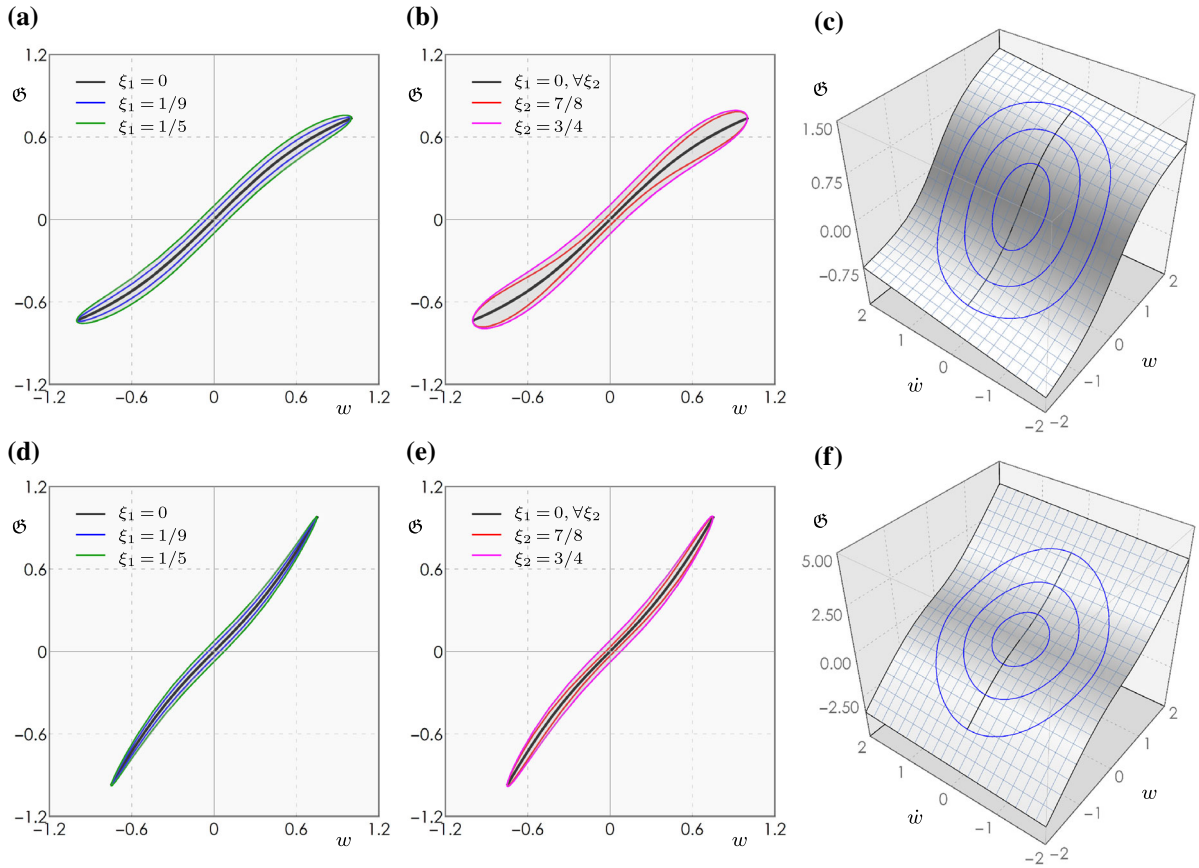

Fig. 2 The constitutive behavior of the ring-resonator coupling for fixed geometric stiffness $\mu = 1/2$: **a**, **b**, **c** softening for small stiffness $\eta = 5/100$; **d**, **e**, **f** hardening for larger stiffness $\eta = 125/100$. Hysteresis loops for (a),(d) $\xi_2 = \xi_3 = 1/2$ and variable ξ_1; (b),(e) $\xi_1 = 1/3$, $\xi_3 = 1$ and variable ξ_2; (c),(f) hysteresis loops and restoring force surface versus displacement and velocity for $\xi_1 = 1/9$, $\xi_2 = \xi_3 = 1/2$

the free wave propagation is governed by the system of second-order ordinary differential equations

$$\begin{aligned} &(1+\varrho^2)\ddot{u} + \varrho^2\ddot{w} + 2\theta(\beta)u = 0, \\ &\varrho^2\ddot{u} + \varrho^2\ddot{w} + G(w,\dot{w};\boldsymbol{\xi}) + F(w;\mu,\eta) = 0 \end{aligned} \tag{10}$$

with $\theta(\beta) := (1-\cos\beta)/2$. Therefore, the nonlinear functions $G(w,\dot{w};\boldsymbol{\xi})$ and $F(w;\mu,\eta)$ can be expressed as Taylor series expansions of the variable w. It is worth noting that the expansion of $F(w;\mu,\eta)$ yields $2\mu w + (\eta-\mu)w^3 + O(w^5)$. Thus 2μ is the linear stiffness coefficient and $\kappa := (\mu-\eta)$ is the cubic stiffness coefficient, which can give rise to either a hardening nonlinearity (if $\kappa < 0$, hence $\eta > \mu$) or a softening nonlinearity (if $\kappa > 0$, hence $\eta < \mu$). On the other hand, the expansion of $G(w,\dot{w};\boldsymbol{\xi})$ delivers $\xi_1(1-\xi_2)\dot{w} + \xi_1\xi_2\xi_3\dot{w}w^2 + O(w^5)$. Therefore, the linear damping coefficient is $\xi := \xi_1(1-\xi_2)$ and is positive if $\xi_1 > 0$ and $\xi_2 < 1$. The coefficient $\zeta := \xi_1\xi_2\xi_3$ scales the cubic nonlinear damping force of the dashpot.

After the expansion, Eq. (10) can be reduced to a first order form via a standard procedure. By introducing the state vector $z := \big(u, w, \dot{u} + \varrho^2(\dot{u}+\dot{w}), \varrho^2(\dot{u}+\dot{w})\big)$ (recall that $\varrho > 0$ by definition), the vector-valued state space governing equations can be cast in the form

$$\dot{\boldsymbol{z}} = \boldsymbol{A}\,\boldsymbol{z} + \varepsilon\boldsymbol{n}(\boldsymbol{z}), \tag{11}$$

where the linear coefficient matrix is

$$\boldsymbol{A} := \begin{pmatrix} 0 & 0 & 1 & -1 \\ 0 & 0 & -1 & \chi \\ -2\theta & 0 & 0 & 0 \\ 0 & -2\mu & \xi & -\xi\chi \end{pmatrix},$$

and the auxiliary parameter $\chi := 1 + \varrho^{-2}$ is fully related to the mass ratio. The ε-scaled vector of nonlinear forces is $\boldsymbol{n} = (0, 0, 0, \mathfrak{g}(z))$, where the nontrivial component is

$$\begin{aligned}\mathfrak{g}(z) &= \xi_1\xi_2\xi_3(z_3 - \chi z_4)z_2^2 + (\mu - \eta)z_2^3 + \text{h.o.t.}\\ &= \zeta(z_3 - \chi z_4)z_2^2 + \kappa z_2^3 + \text{h.o.t.}\end{aligned} \tag{12}$$

and the notable relation $\dot{w} = z_3 - \chi z_4$ has been employed. It is worth noting that the cubic cut-off $\mathfrak{g}(z)^{[\leq 3]}$ of the nonlinearity is adopted in the following, so that terms of order higher than 3 are disregarded. The parameter ε has the meaning of scaling parameter "introduced to study small amplitude solutions", and it is straightforwardly defined via the standard substitution $z \leftarrow \sqrt{\varepsilon}z$. This point is crucial for interpreting the outcomes of the numerical experiments.

From the physical viewpoint, the case of weak dissipation (small linear and nonlinear damping terms) will be identified by small and positive ξ-values. In this respect, attention is restricted to the case in which none of the eigenvalues λ_j $(j = 1, ..., 4)$ of the spectrum of $\boldsymbol{A}$ are purely real. Despite the roots of the characteristic quartic polynomial of $\boldsymbol{A}$ could be written explicitly, it is easy to realize that an exact characterization of the hyperbolicity of the origin would require quite involved expressions. The following statement, proposing a sufficient condition, is a compromise allowing to deal with a straightforward constraint on the model parameters:

Proposition 2.1 (A sufficient condition for the existence of non-purely real eigenvalues). *Suppose that*

$$\xi^2 < 4(\mu\chi + \theta)\min\{\chi^{-2}, \mu\varrho^2\theta^{-1}\}, \tag{13}$$

and recall that $\theta \neq 0$. *Then*

$$\lambda_{1,2} = \alpha_1 \pm i\beta_1, \qquad \lambda_{3,4} = \alpha_2 \pm i\beta_2, \tag{14}$$

with $\alpha_{1,2} \in \mathbb{R}$ *and* $\beta_{1,2} \in \mathbb{R}$. *Moreover,* $\alpha_{1,2} \leq 0$ $(\alpha_{1,2} = 0 \Leftrightarrow \xi = 0)$ *and* $\beta_{1,2} > 0$, *i.e.,* $\lambda_j \in \mathbb{C} \setminus \{0\}$.

See Appendix for the proof.

Remark 2.1 Inequality (13) is always satisfied for sufficiently small ξ and it will be assumed to hold here and henceforth. It can be anticipated that the eigenvalues, as well as the associated eigenvectors (and other related quantities), lend themselves to an interesting perturbation expansion in terms of ξ. See Prop. 5.1 and its proof.

Once the four eigenvalues (here assumed to be simple) are known, the complex-valued eigenvector $\boldsymbol{v}_j$ associated to the eigenvalue λ_j can be determined

$$\boldsymbol{v}_j := \begin{pmatrix} 1 \\ (2\theta - 2\chi\theta - \chi\lambda_j^2)/\lambda_j^2 \\ -2\theta/\lambda_j \\ (2\theta + \lambda_j^2)/\lambda_j \end{pmatrix}, \tag{15}$$

where a suitable z_1-unitary amplitude normalization has been adopted. Therefore, it is convenient to introduce the linear modal transformation

$$\boldsymbol{z} = \boldsymbol{\Psi}\boldsymbol{x}, \qquad \boldsymbol{\Psi} = (\boldsymbol{v}_1, \boldsymbol{v}_2, \boldsymbol{v}_3, \boldsymbol{v}_4) \tag{16}$$

to express the system dynamics in normal coordinates $\boldsymbol{x}$. Accordingly, upon substitution of Eq. (16) into Eq. (11) and premultiplication of both sides by $\boldsymbol{\Psi}^{-1}$, the ensuing differential system is cast in diagonal form

$$\dot{\boldsymbol{x}} = \boldsymbol{\Lambda}\boldsymbol{x} + \varepsilon\boldsymbol{f}(\boldsymbol{x}), \tag{17}$$

with the diagonal matrix $\boldsymbol{\Lambda} = \text{diag}(\lambda_1, \lambda_2, \lambda_3, \lambda_4)$ and the nonlinear vector field

$$\begin{aligned}\boldsymbol{f}(\boldsymbol{x}) &:= \boldsymbol{\Psi}^{-1}\boldsymbol{n}(\boldsymbol{\Psi}\boldsymbol{x}) = \boldsymbol{\Psi}^{-1}(0, 0, 0, \mathfrak{g}^{[\leq 3]}(\boldsymbol{\Psi}\boldsymbol{x}))^\top\\ &=: \mathfrak{g}^{[\leq 3]}(\boldsymbol{\Psi}\boldsymbol{x})(r_1, r_2, r_3, r_4)^\top.\end{aligned} \tag{18}$$

where superscript $\top$ denotes the transpose. It is straightforward to show that, as the rows of $\boldsymbol{\Psi}$ are complex-conjugate, so are the columns of $\boldsymbol{\Psi}^{-1}$. This implies, $r_1 = \bar{r}_2$ and $r_3 = \bar{r}_4$, where the overbar indicates the complex conjugate. It may be worth noting that the eigenvalue and eigenvector matrices $\boldsymbol{\Lambda}$ and $\boldsymbol{\Psi}$ are complex-valued in the general case, since the mechanical parameters (in particular, the dissipation terms) are not higher order terms, as it typically happens in other perturbation problems.

3 Lie series operators and Hamiltonian perturbation theory: a short overview

Perturbation methods are flexible and efficient mathematical tools to determine analytical—asymptotically approximate—solutions for nonlinear dynamic problems. Within the context of wave propagation in periodic materials and structures, different perturbation techniques have been employed to study the nonlinear dispersion properties of harmonic waves, including the modified harmonic balance (with ordering of the harmonic amplitudes) [53], Lindstedt-Poincaré [55,56] and the method of multiple scales [22,42,43,45,46].

With respect to this well-established framework, the original contribution offered by the present work consists in approaching the damped free propagation of nonlinear waves by means of the Hamiltonian perturbation theory. To this end, the main elements of the Lie series operator approach to Hamiltonian perturbation theory are recalled here for the sake of a better readability, as well as to fix the notational setting. A comprehensive discussion of this subject can be found in [70].

Given $n \geq 1$, the space $\mathcal{F}$ of smooth functions defined on $\mathbb{M} \subseteq \mathbb{R}^{2n}$, endowed with canonical coordinates $(\boldsymbol{y}, \boldsymbol{x})$, is considered. Hamiltonian perturbation theory in the nearly-integrable context, usually deals with dynamic systems defined via the Hamiltonian:

$$H = H_0 + \varepsilon H_1,$$

where H_0 is the *integrable part* and εH_1 is interpreted as a *perturbation*, being $\varepsilon > 0$ a "small" parameter.

The core idea is to seek a canonical transformation $\mathcal{N} : (\boldsymbol{y}, \boldsymbol{x}) \to (\boldsymbol{y}', \boldsymbol{x}')$, i.e., a transformation which preserves the Hamiltonian structure[1], in such a way that the Hamiltonian function in the new set of variables $H'(\boldsymbol{y}', \boldsymbol{x}')$ is cast into a form $H' = H'_0 + S$. The "remainder" S is ideally $O(\varepsilon^2)$ but it can possibly include some $O(\varepsilon)$ terms (as in the present case, see Sect. 4). It is well known that, even in the "best" case in which $S = O(\varepsilon^2)$, the possibility to iterate the above described procedure in order to obtain $O(\varepsilon^n)$ remainders (with n arbitrarily large), is *generically* excluded.

Within this mathematical framework, the *Lie series operator* is defined as

$$\exp(\mathcal{L}_g) := \mathrm{Id} + \sum_{s=1}^{+\infty} \frac{1}{s!} \mathcal{L}_g^s, \qquad g \in \mathcal{F},$$

where $\mathcal{L}_g \cdot := \{\cdot, g\}$ and the classical Poisson brackets

$$\{\hat{f}, \hat{h}\} \equiv \sum_{i=1}^{n} \left[\partial_{x_i} \hat{f} \partial_{y_i} \hat{h} - \partial_{y_i} \hat{f} \partial_{x_i} \hat{h} \right], \qquad \forall \hat{f}, \hat{h} \in \mathcal{F}$$

has been introduced. As anticipated in the foreword, the Lie series operator has been shown to play a remarkable role in the context of perturbation theory. In fact, the transformation of variables generated by the Lie series operator

$$(\boldsymbol{y}, \boldsymbol{x}) := \exp(\mathcal{L}_g)(\boldsymbol{y}', \boldsymbol{x}'), \tag{19}$$

can be proven to be canonical and, remarkably, possesses an explicit form [70, Chap. 4].

[1] Knowingly, a sufficient and necessary condition of canonicity is that the Jacobian matrix of the transformation is symplectic.

Within this context, a mathematical tool to construct the so-called "generating function" g is provided by the *Gröbner exchange theorem*, stating that

$$H|_{(\boldsymbol{y},\boldsymbol{x}):=\exp(\mathcal{L}_g)(\boldsymbol{y}',\boldsymbol{x}')} = \left[\exp(\mathcal{L}_g) H\right]_{(\boldsymbol{y},\boldsymbol{x})=(\boldsymbol{y}',\boldsymbol{x}')}, \tag{20}$$

see also [76]. More precisely, let $g := \varepsilon \tilde{g}$ and require $\exp(\mathcal{L}_{\varepsilon\tilde{g}}) H = H_0 + S$, where S has been defined earlier. It is possible to check that, at the first order in ε, this leads to the *homological equation*

$$\mathcal{L}_{\tilde{g}} H_0 + H_1 = 0. \tag{21}$$

Equations of this form play a central role in the perturbation framework. Their resolvability strongly depends on the problem at hand and related internal resonance phenomena (as shown later in Sect. 4).

To the purposes of the present work, it may be sufficient to point out (see, for instance, [77]) that every system of ODEs $\dot{\boldsymbol{x}} = \boldsymbol{v}(\boldsymbol{x})$, $\boldsymbol{x} \in \mathbb{R}^n$ can be interpreted as (part of the) canonical equations of the Hamiltonian system given by

$$\mathcal{H} := \boldsymbol{y} \cdot \boldsymbol{v}(\boldsymbol{x}),$$

in the extended phase space $\mathbb{M} \ni (\boldsymbol{y}, \boldsymbol{x})$. This approach will be profitably used later in Sect. 4 to carry out the perturbation analysis in the Hamiltonian setting.

4 A first-order perturbation analysis

In order to apply the Hamiltonian perturbation theory to the mechanical problem under investigation, the governing Eq. (17) can also be expressed in the component form

$$\dot{x}_j = \lambda_j x_j + \varepsilon f_j(\boldsymbol{x}), \tag{22}$$

from which the following Hamiltonian function can be defined

$$H(\boldsymbol{y}, \boldsymbol{x}) := \sum_{j=1}^{4} \lambda_j y_j x_j + \varepsilon \tilde{\mathfrak{g}}(\boldsymbol{x}) \sum_{j=1}^{4} r_j y_j,$$

with

$$\tilde{\mathfrak{g}}(\boldsymbol{x}) := \mathfrak{g}^{[\leq 3]}(\boldsymbol{\Psi}\boldsymbol{x}) = \sum_{|\boldsymbol{\nu}|=3} \gamma_{\boldsymbol{\nu}} P_{\boldsymbol{\nu}}(\boldsymbol{x}), \tag{23}$$

where the product $P_{\boldsymbol{\nu}}(\boldsymbol{x}) := \Pi_{j=1}^{4} x_j^{\nu_j}$ has been introduced and $\boldsymbol{\nu}$ is a vector of $\mathbb{N}^4$ with each element being one of the integer numbers $0, 1, 2, 3$ and such that $|\boldsymbol{\nu}| = 3$.

Remark 4.1 The determination of the coefficients $\gamma_{\boldsymbol{\nu}}$ in terms of the Taylor coefficients of $\boldsymbol{n}(z)$ is not straightforward, but requires the solution of an implicit algebraic equation. The full expression is given in Appendix.

Given the structure of the Hamiltonian, by following the lines of [59], a generating function of the form

$$g = \varepsilon \sum_{j=1}^{4} y_j \mathcal{C}_j(\boldsymbol{x}),$$
$$\mathcal{C}_j(\boldsymbol{x}) := \sum_{|\boldsymbol{\nu}|=3} c_{\boldsymbol{\nu}}^{(j)} P_{\boldsymbol{\nu}}(\boldsymbol{x}), \tag{24}$$

is sought, where the coefficients $c_{\boldsymbol{\nu}}^{(j)}$ are unknowns. In this respect, the homological equation of the first perturbation step leads to

$$\left\{ g, \sum_{j=1}^{4} \lambda_j y_j x_j \right\} = \tilde{\mathfrak{g}}(\boldsymbol{x}) \sum_{j=1}^{4} r_j y_j$$

which, after a suitable rearrangement of terms in its left hand side, yields

$$\sum_{j=1}^{4} y_j \sum_{|\boldsymbol{\nu}|=3} (\boldsymbol{\lambda} \cdot \boldsymbol{\nu} - \lambda_j) c_{\boldsymbol{\nu}}^{(j)} P_{\boldsymbol{\nu}}(\boldsymbol{x}) = \sum_{j=1}^{4} r_j y_j \sum_{|\boldsymbol{\nu}|=3} \gamma_{\boldsymbol{\nu}} P_{\boldsymbol{\nu}}(\boldsymbol{x})$$

where $\boldsymbol{\lambda} = (\lambda_1, \lambda_2, \lambda_3, \lambda_4)$. Consequently, the obtained set of equations gives rise to the expression for the coefficients of the generating function

$$c_{\boldsymbol{\nu}}^{(j)} = \frac{r_j \gamma_{\boldsymbol{\nu}}}{\boldsymbol{\lambda} \cdot \boldsymbol{\nu} - \lambda_j} \tag{25}$$

(see, e.g., [78] for a direct derivation without using the Hamiltonian formalism).

The behavior of the denominator $\boldsymbol{\lambda} \cdot \boldsymbol{\nu} - \lambda_j$ is known to play a crucial role in perturbation theory. In particular, as known, a general obstruction to a normalization up to an arbitrarily high order lies in the fact that the quantity $L_j(s) := \{\inf_{|\boldsymbol{\nu}|=s} |\boldsymbol{\lambda} \cdot \boldsymbol{\nu} - \lambda_j|\}$ approaches rapidly zero as s increases (condition known as *small divisors*), thus jeopardizing the convergence of the asymptotic series in the parameter space (see also [70]). However, as far as the first normalization step is concerned, recalling that ξ is a strictly positive constant and independent of ε, it is sufficient to assume the following Ansatz.

Hypothesis 4.1 *(non-resonance conditions): The definition* $\Pi_{i,j}(\sigma) := \{(\beta_1, \beta_2) \in [0, +\infty)^2 : \beta_i = \sigma \beta_j\}$ *is introduced. It is supposed that* $(\beta_1, \beta_2) \notin \mathfrak{R}$*, where*

$$\mathfrak{R} := \Pi_{2,1}(0) \cup \Pi_{2,1}(1/3) \cup \Pi_{2,1}(1) \cup \Pi_{2,1}(3) \cup \Pi_{1,2}(0),$$

is the "internal resonance manifold".

Such a manifold describes conditions on the imaginary part of the eigenvalues (i.e., linear wavefrequencies) according to which internal resonances (also called *autoparametric* resonances) may occur between linear waveforms characterized by different polarizations [13]. From the physical viewpoint, internal resonance conditions may activate significant energy transfers between the periodic lattice and its local resonators.

A special attention should be devoted to the fact that $\lim_{\xi \to 0} \alpha_{1,2} = 0$ (more on this is reported in Sect. 6). For instance, if $j = 1$, one has

$$\boldsymbol{\lambda} \cdot \boldsymbol{\nu} - \lambda_1 = \alpha_1(\nu_1 + \nu_2 - 1) + i\beta_1(\nu_1 - \nu_2 - 1) + \alpha_2(\nu_3 + \nu_4) + i\beta_2(\nu_3 - \nu_4).$$

Clearly, amongst those $\boldsymbol{\nu}$ such that $|\boldsymbol{\nu}| = 3$, either in the case $\boldsymbol{\nu} = (1, 0, 1, 1)$ or $\boldsymbol{\nu} = (2, 1, 0, 0)$ one finds that $\boldsymbol{\lambda} \cdot \boldsymbol{\nu} - \lambda_1$ vanishes as $\xi \to 0$. By proceeding in a similar way, one obtains three more pairs of values to be excluded as j varies, say $\boldsymbol{\nu}^a$ and $\boldsymbol{\nu}^b$. The whole set of $\boldsymbol{\nu}$'s to be excluded, which will be denoted with $\mathcal{S}_r$, is collected in Table 1. Knowingly, the previous terms cannot be removed with the normalization procedure but remain in the transformed Hamiltonian as "resonance" terms. As a consequence, by following the procedure outlined in Sect. 3, it is possible to introduce the new set of variables $(\boldsymbol{X}, \boldsymbol{Y})$ (implicitly) defined by the transformation $\mathcal{N}_g : (\boldsymbol{X}, \boldsymbol{Y}) \to (\boldsymbol{x}, \boldsymbol{y})$, according to which

$$(\boldsymbol{x}, \boldsymbol{y}) = \mathcal{L}_g(\boldsymbol{x}, \boldsymbol{y})|_{(\boldsymbol{x},\boldsymbol{y})=(\boldsymbol{X},\boldsymbol{Y})} + O(\varepsilon^2), \tag{26}$$

where g is given by

$$g = \varepsilon \sum_{j=1}^{4} y_j r_j \left[\sum_{\substack{|\boldsymbol{\nu}|=3 \\ \boldsymbol{\nu} \notin \mathcal{S}_r}} \frac{\gamma_{\boldsymbol{\nu}} P_{\boldsymbol{\nu}}(\boldsymbol{x})}{\boldsymbol{\lambda} \cdot \boldsymbol{\nu} - \lambda_j} \right],$$

i.e., from (24) and (25). As minor comparative remark, the issue of small divisors in resonant or quasi-resonant conditions is known to occur also in other perturbation schemes, like – for instance – the straightforward-expansion method. On the contrary, other perturbation schemes, such as the method of multiple scales, deliver

Table 1 The set $\mathcal{S}_r$ of $\boldsymbol{\nu}$-values to be excluded

j	$\boldsymbol{\nu}^a$	$\boldsymbol{\nu}^b$
1	(1,0,1,1)	(2,1,0,0)
2	(0,1,1,1)	(1,2,0,0)
3	(0,0,2,1)	(1,1,1,0)
4	(0,0,1,2)	(1,1,0,1)

solutions that are systematically free of small-divisor terms, since the resonant terms are conveniently treated a priori by imposing proper solvability conditions on the perturbation equations [79,80].

Remark 4.2 It is possible to show that the $\boldsymbol{x}$ components of the transformation formulae given by (26) are, consistently, functions of $\boldsymbol{X}$ only so that (26) can be used directly on (11). In other words, one can "forget to have used the Hamiltonian formalism" at this point, as the $\boldsymbol{Y}$ variables will never appear in the transformed system. See [59] for the proof.

In this way, the transformed Hamiltonian

$$\tilde{H} := \exp(\mathcal{L}_g) H|_{(\boldsymbol{x},\boldsymbol{y})=(\boldsymbol{X},\boldsymbol{Y})},$$

recall (20), reads as

$$\begin{aligned}\tilde{H} = &\sum_{j=1}^{4} \lambda_j Y_j X_j \\ &+\varepsilon r_1 Y_1 (\gamma_{(1,0,1,1)} X_1 X_3 X_4 + \gamma_{(2,1,0,0)} X_1^2 X_2) \\ &+\varepsilon r_2 Y_2 (\gamma_{(0,1,1,1)} X_2 X_3 X_4 + \gamma_{(1,2,0,0)} X_1 X_2^2) \\ &+\varepsilon r_3 Y_3 (\gamma_{(0,0,2,1)} X_3^2 X_4 + \gamma_{(1,1,1,0)} X_1 X_2 X_3) \\ &+\varepsilon r_4 Y_4 (\gamma_{(0,0,1,2)} X_3 X_4^2 + \gamma_{(1,1,0,1)} X_1 X_2 X_4) \\ &+O(\varepsilon^2).\end{aligned}$$

Such a $\tilde{H}$ generates the set of canonical equations

$$\begin{aligned}\dot{X}_1 &= X_1 \left[\lambda_1 + \varepsilon r_1 (\gamma_{(1,0,1,1)} X_3 X_4 + \gamma_{(2,1,0,0)} X_1 X_2)\right] \\ \dot{X}_2 &= X_2 \left[\lambda_2 + \varepsilon r_2 (\gamma_{(0,1,1,1)} X_3 X_4 + \gamma_{(1,2,0,0)} X_1 X_2)\right] \\ \dot{X}_3 &= X_3 \left[\lambda_3 + \varepsilon r_3 (\gamma_{(0,0,2,1)} X_3 X_4 + \gamma_{(1,1,1,0)} X_1 X_2)\right] \\ \dot{X}_4 &= X_4 \left[\lambda_4 + \varepsilon r_4 (\gamma_{(0,0,1,2)} X_3 X_4 + \gamma_{(1,1,0,1)} X_1 X_2)\right]\end{aligned} \tag{27}$$

obtained upon disregarding $O(\varepsilon^2)$ terms.

5 A suitable set of coordinates and nonlinear spectra

In order to emphasizes the geometric features of equations (27), they can be cast in a suited set of coordinates. Firstly, it is convenient to cast such a system into a real form. To this end, the (classical) transformation

$$\begin{pmatrix} X_{2j-1} \\ X_{2j} \end{pmatrix} = \frac{1}{\sqrt{2}} \begin{pmatrix} 1 & i \\ 1 & -i \end{pmatrix} \begin{pmatrix} V_{2j-1} \\ V_{2j} \end{pmatrix}, \qquad j = 1, 2, \tag{28}$$

is considered. This procedural expedient can comparatively be associated to the transformation into real-valued polar coordinates of the complex-valued modulation amplitudes in the method of multiple scales. After slight manipulations and retaining terms up to the first-order terms in ε, Eq. (27) take the form

$$\begin{aligned}\dot{V}_{2j-1} &= \alpha_j V_{2j-1} - \beta_j V_{2j} \\ &\quad + \tfrac{1}{2}\varepsilon \left\{ V_{2j-1} \left[M_{1,2}^{(j)} (V_1^2 + V_2^2) + M_{3,4}^{(j)} (V_3^2 + V_4^2) \right] \right. \\ &\quad \left. - V_{2j} \left[N_{1,2}^{(j)} (V_1^2 + V_2^2) + N_{3,4}^{(j)} (V_3^2 + V_4^2) \right] \right\}, \\ \dot{V}_{2j} &= \beta_j V_{2j-1} + \alpha_j V_{2j} \\ &\quad + \tfrac{1}{2}\varepsilon \left\{ V_{2j-1} \left[N_{1,2}^{(j)} (V_1^2 + V_2^2) + N_{3,4}^{(j)} (V_3^2 + V_4^2) \right] \right. \\ &\quad \left. + V_{2j} \left[M_{1,2}^{(j)} (V_1^2 + V_2^2) + M_{3,4}^{(j)} (V_3^2 + V_4^2) \right] \right\},\end{aligned} \tag{29}$$

with $j = 1, 2$, where

$$\begin{aligned} M_{1,2}^{(1)} &= \Re(r_1 \gamma_{(2,1,0,0)}), & M_{3,4}^{(1)} &= \Re(r_1 \gamma_{(1,0,1,1)}), \\ M_{1,2}^{(2)} &= \Re(r_3 \gamma_{(0,0,2,1)}), & M_{3,4}^{(2)} &= \Re(r_3 \gamma_{(1,1,0,1)}), \\ N_{1,2}^{(1)} &= \Im(r_1 \gamma_{(2,1,0,0)}), & N_{3,4}^{(1)} &= \Im(r_1 \gamma_{(1,0,1,1)}), \\ N_{1,2}^{(2)} &= \Im(r_3 \gamma_{(0,0,2,1)}), & N_{3,4}^{(2)} &= \Im(r_3 \gamma_{(1,1,0,1)}). \end{aligned} \tag{30}$$

The damping term can now be "removed" by using the transformation

$$(V_{2j-1}, V_{2j}) = e^{\alpha_j \tau} (U_{2j-1}, U_{2j}), \quad j = 1, 2. \tag{31}$$

In this way the motion can be meaningfully represented by means of polar-like coordinates

$$(U_{2j-1}, U_{2j}) = \sqrt{2 I_j} (\cos\varphi_j, \sin\varphi_j), \qquad j = 1, 2, \tag{32}$$

which represent a suitable coordinate set $(\boldsymbol{I}, \boldsymbol{\varphi})$ of time-dependent *action-angle* (I_j, φ_j)-variables (with $j = 1, 2$) for the unperturbed motion. By introducing the transformations (31) and (32), Eq. (29) becomes

$$\dot{I}_j = 2\varepsilon I_j \left[M_{1,2}^{(j)} e^{2\alpha_1 \tau} I_1 + M_{3,4}^{(j)} e^{2\alpha_2 \tau} I_2 \right] + O(\varepsilon^2),$$

$$\dot{\varphi}_j = \beta_j + \varepsilon \left[N_{1,2}^{(j)} e^{2\alpha_1 \tau} I_1 + N_{3,4}^{(j)} e^{2\alpha_2 \tau} I_2 \right] + O(\varepsilon^2) \tag{33}$$

and regulate the time-dependence of the action-angle coordinates in a manner that is formally similar to the ordinary differential equations governing the amplitude modulation in the method of multiple scales. From the geometrical viewpoint, in this set of coordinates the unperturbed solutions are naturally interpreted as a flow on the 2-torus $\mathbb{T}^2$ (that is, the two-dimensional torus expressed as product of two circles) with frequencies β_1 and β_2, i.e.

$$\begin{aligned} &I_j(\tau) = I_j(0), \\ &\varphi_j(\tau) = \varphi_j(0) + \beta_j \tau, \quad j = 1, 2. \end{aligned} \tag{34}$$

Furthermore, if $\alpha_{1,2} < 0$, it is clear that the nonlinear corrections to the frequencies β_j will vanish as $\tau \to +\infty$. In fact, for any set of initial conditions, if $\xi > 0$, no matter how small, the system loses energy because of the dissipation, so that its solutions will be absorbed by any arbitrarily small open neighborhood of the hyperbolic equilibrium located at the origin. Here, the effect of the nonlinearity becomes weaker and weaker as the radius of such a neighborhood shrinks over time. Moreover, one obtains from the first of (33) that $I_j(\tau) = I_j(0) + O(\varepsilon)$, so that, by substituting the latter in the second of (33), one gets

$$\begin{aligned} \dot{\varphi}_j = \ & \beta_j + \varepsilon \left[N_{1,2}^{(j)} e^{2\alpha_1 \tau} I_1(0) + N_{3,4}^{(j)} e^{2\alpha_2 \tau} I_2(0) \right] \\ & + O(\varepsilon^2). \end{aligned} \tag{35}$$

This equation shows that the time-independent coefficients $N_{1,2}^{(j)}$ and $N_{3,4}^{(j)}$ regulate, in the jth nonlinear waveform, the nonlinear frequency corrections due to the initial conditions on the acoustic ($j = 1$) and optical ($j = 2$) waves. Furthermore, for any fixed τ, the spectra can be interpreted as action-dependent functions $\mathcal{S}_{j,\varepsilon} = \mathcal{S}_{j,\varepsilon}(I_j(0))$, i.e., surfaces parametrized by the two constants $I_j(0)$ and appearing as perturbations of the $I_j(0)$-independent, or "flat", surfaces $\mathcal{S}_{j,0} \equiv \beta_j$ representing the dispersion curves.

It is worth remarking that the two coefficients $N_{1,2}^{(j)}, N_{3,4}^{(j)}$, known as *effective nonlinearity coefficients*, incorporate the contributions of all the mechanical parameters appearing in the problem formulation, and depend also on the wavenumber β. Whenever one of these coefficients is positive (or negative), the associated frequency correction is softening (or hardening). Variations of these coefficients over the meaningful range of the (κ, ζ)-parameters are shown in Fig. 3. As expected, the coefficients are negative (yellow light red) for positive values of κ (softening) and are positive (orange and dark red) for negative κ (hardening). This dominant scenario is slightly perturbed by the effects of the nonlinear viscosity ζ, which become nonnegligible only for vanishing nonlinear stiffness ($\kappa \simeq 0$). Indeed, while the sensitivity with respect to the nonlinear stiffness coefficients is significant, much less sensitivities are exhibited with respect to the linear viscosity coefficient ξ_1 (here not reported for the sake of conciseness), as well as with respect to the nonlinear viscosity coefficient ζ.

Figure 4 offers a possible representation of the spectra $\mathcal{S}_{j,\varepsilon}$ for fixed parameters ($\mu = 1/2$, $\varrho = 48/10$, $\eta = 5/100$, $\boldsymbol{\xi} = (1/10, 1/2, 1/2)$) and for $\varepsilon = 10^{-2}$ in the $(|\boldsymbol{I}(0)|, \beta)$-space at different time instants (Fig. 4a-c), under the additional constraint $I_1(0) = I_2(0)$. The lower-frequency surface $\mathcal{S}_{1,\varepsilon}$ and higher-frequency surface $\mathcal{S}_{2,\varepsilon}$ describe the nonlinear and time-dependent dispersion properties of the metamaterial. The dependence of the surfaces on the wavenumber β and initial action norm $|\boldsymbol{I}(0)|$ is noticeable. The chosen ε-value (condition (36) holds) corresponds to solutions of $O(10^{-1})$ magnitude (see Sect. 2). Note that the surfaces tend to become independent of the initial energy for large times. This means that the metamaterial tends to be governed by a linear behavior for longer times due to the effects of dissipation, which induces an exponential decay of the oscillation amplitudes (related to the square root of the action norm) assigned as initial conditions. For the sake of completeness, the curve defined by the locus $\Gamma = (\beta_1(\theta), \beta_2(\theta))$ for $\theta \in (0, 1)$ is verified "a posteriori" to be away from the resonant set $\mathfrak{R}$, as shown in Fig. 4d (see also Rem. 5.1). The corresponding zero dissipation limit (obtained for $\xi_1 = 0$) is reported in Fig. 5a. In this limit case, the nonlinear spectrum is recognized to be amplitude-dependent but time-independent, as expected for non-dissipative systems and consistently with [22]. The corresponding linear spectrum (i.e. dispersion curves) is also obtainable, as section of the time-independent spectrum for $\boldsymbol{I}(0) = 0$ (Fig. 5b). The corresponding linear waveforms can be proven to be real-valued [22]. The unit-norm waveforms represented over the unit circle of the (u, w)-space allow to distinguish the different polarizations of the linear nondissipative waves propagating at selected wavenumbers [13]. A nonnegligible partic-

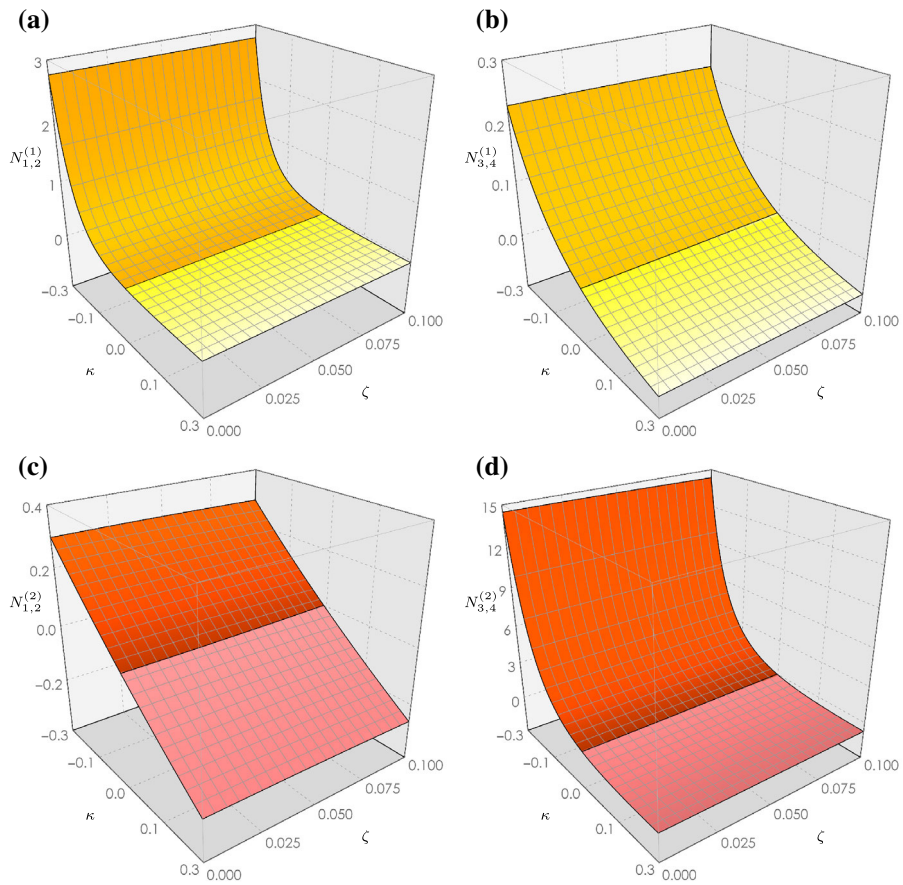

Fig. 3 Variations of the effective nonlinearity coefficients in the wave frequencies over the (κ, ζ)-parameter space: **a**–**b** acoustic coefficients and **c**–**d** optical coefficients

ipation of the w-component in the waveform means significant activation of the ring-resonator coupling.

Figure 6 shows the backbone curves $\sigma_j = \dot{\varphi}_j/\dot{\varphi}_j^\circ$ (where $\dot{\varphi}_j^\circ$ is the frequency $\dot{\varphi}_j$ evaluated at $\boldsymbol{I}(0) = 0$ for $\xi_1 = 0$, corresponding to the *undamped linear* frequency) at the limit of short wavelengths ($\beta = \pi$) for the conservative case (colored lines). Due to nonlinearities, the acoustic and optical frequencies show a marked dependence on the oscillation amplitude (related to the square root of the action norm). Fixing different sets of mechanical parameters, a *heavy* metamaterial shows a softening behavior (Fig. 6a, b), while a *light* metamaterial shows a hardening behavior (Fig. 6c, d). The time-independent non-dissipative case is also compared with the dissipative case at different times (gray lines). The interesting feature is that the dissipation delivered by the dashpots reduces the softening/hardening effect induced by the nonlinearities until it becomes vanishing (that is, nonlinear damped frequency tending to the damped linear frequency) for sufficiently long times.

While this result is expected from a purely physical standpoint, its quantification as to the time window over which the nonlinearity is dominant is a key contribution here provided.

Remark 5.1 Amongst the other parameters, the imaginary parts $\beta_{1,2}$ depend on θ. If the remaining parameters are supposed to be fixed once and for all, as θ varies in $(0, 1)$, the planar curve $(\beta_1(\theta), \beta_2(\theta))$ might cross one or more resonant lines belonging to $\mathfrak{R}$. Clearly, this would not satisfy Hyp. 4.1, so that the whole perturbative argument and, in particular, expression (35) itself, would break down.

In the light of this possibility, it is important to stress that, despite a machine-based ("a posteriori") validation would be straightforward (e.g., by comparing the curve $(\beta_1(\theta), \beta_2(\theta))$ with $\mathfrak{R}$), it is not easy to establish "a priori" conditions in order to avoid such a phenomenon. However, if one supposes that the dissipation size ξ is "sufficiently small", an easily checkable condition can be derived for this purpose:

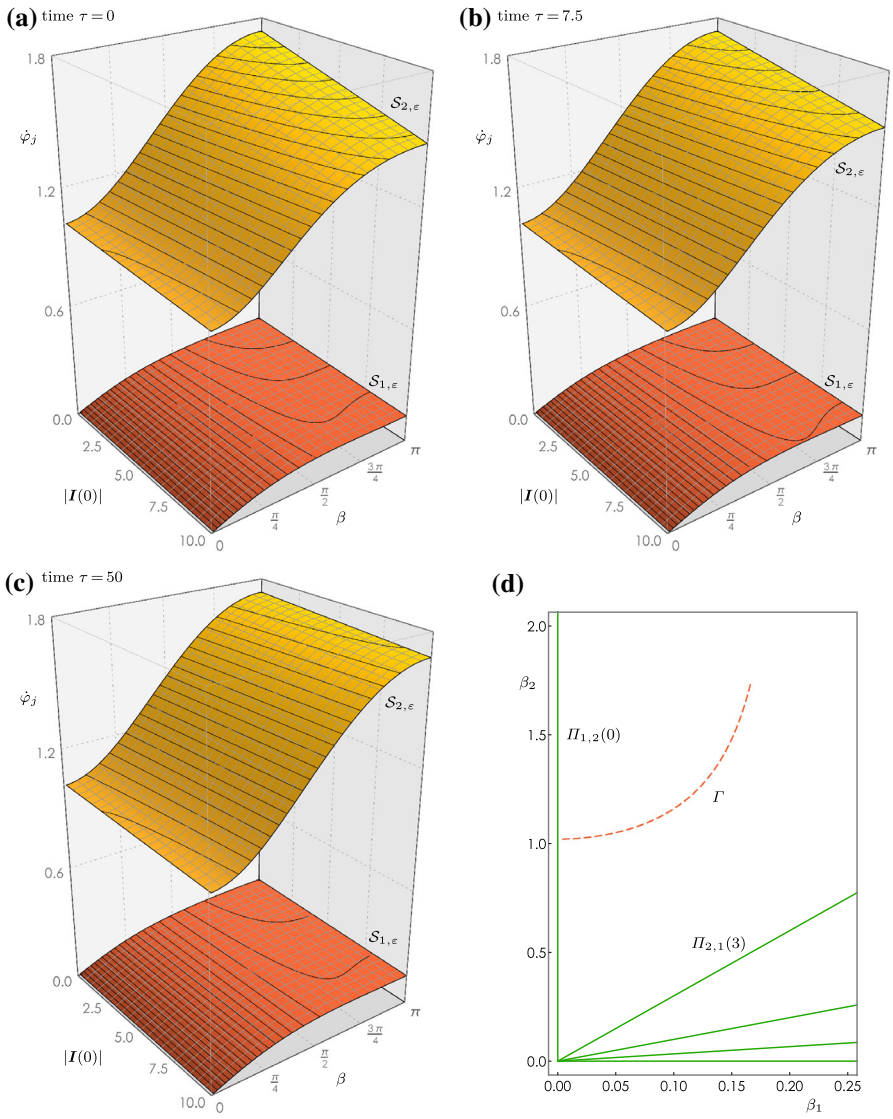

Fig. 4 Nonlinear time-dependent spectra of the 1D metamaterial lattice with $\mu = 1/2$, $\varrho = 48/10$, $\eta = 5/100$, $\boldsymbol{\xi} = (1/10, 1/2, 1/2)$ for $\varepsilon = 10^{-2}$ in the $(|\boldsymbol{I}(0)|, \beta)$-space for different time instants: **a** $\tau = 0$; **b** $\tau = 7.5$; **c** $\tau = 50$; **d** curve Γ for the frequencies β_j obtained for the chosen parameters, as $\theta \in (0, 1)$ (red dashed line), compared with the resonant set $\mathfrak{R}$ (green lines). (Color figure online)

Proposition 5.1 (parametric condition for no internal resonances and eigenvalues expansion in the weak dissipation case). *Assume*

$$\varrho^2 > 100/(9\mu). \tag{36}$$

Then, by setting $\Theta := \sqrt{(\mu\chi + \theta)^2 + 4\theta\mu(1 - \chi)}$, *one has* $\Theta \in ((4/5)\mu, \mu\chi + \theta)$ *and the following expansions hold:*

$$\begin{aligned} \alpha_{1,2} &= -a_{1,2}\xi + O(\xi^2), \\ \beta_{1,2} &= \sqrt{b_{1,2}} + O(\xi^2), \end{aligned} \tag{37}$$

where

$$a_{1,2} = \left[\chi\Theta \pm (\chi\theta - 2\theta - \mu\chi^2)\right]/(4\Theta), \tag{38}$$

$$b_{1,2} = \mu\chi + \theta \mp \Theta. \tag{39}$$

In particular, one obtains for $j, k = 1, 2$,

$$M^{(k)}_{2j-1,2j} = O(\xi). \tag{40}$$

Moreover, for sufficiently small ξ,

$$\{(\beta_1(\theta), \beta_2(\theta)) : \theta \in (0, 1)\} \cap \mathfrak{R} = \emptyset, \tag{41}$$

i.e., no internal resonances occur for any value of θ.

The proof of Prop. 5.1 is reported in Appendix. Furthermore, the approximation of the resonant subset $\Pi_{1,2}(3)$ in the parameters space (θ, χ, μ), as can be obtained by using Prop. 5.1, is portrayed in Fig. 7. Away from the approximated subset $\Pi_{1,2}(3)$ (i.e., 3:1 internal

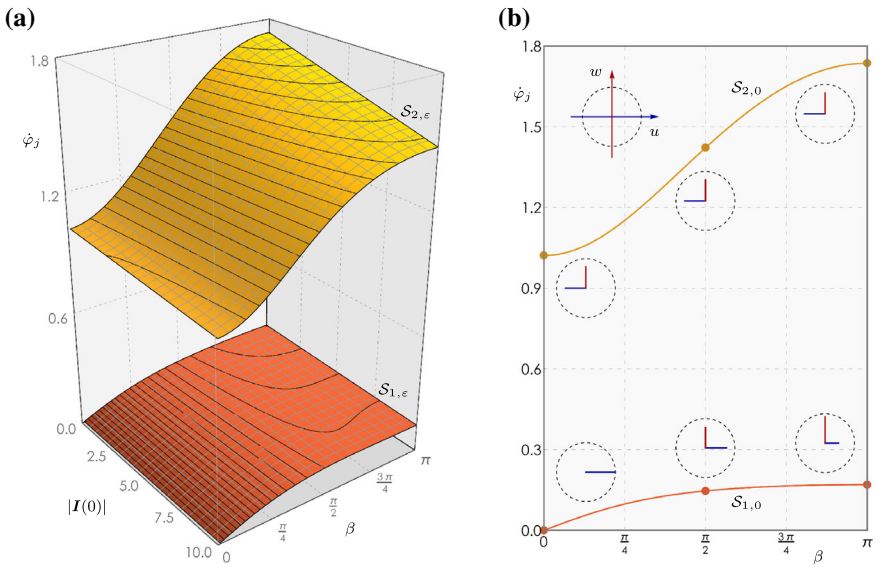

Fig. 5 Nonlinear time-independent spectra of the 1D metamaterial lattice with $\mu = 1/2$, $\varrho = 48/10$, $\eta = 5/100$, for $\varepsilon = 10^{-2}$ in the $(|\boldsymbol{I}(0)|, \beta)$-space (i.e., the zero dissipation limit for $\xi_1 = 0$): **a** nonlinear spectrum; **b** linear spectrum (i.e., intersection of the nonlinear spectra with the plane $|\boldsymbol{I}(0)| = 0$) and the polarization of waveforms for selected wavenumbers

resonance), the locus Γ of (θ, χ, μ)-parameters associated with the spectra reported in Fig. 4 is represented by the dashed red line.

Remark 5.2 It is worth stressing that such a result is not needed if θ is chosen as a *fixed* value (as in the computations of Sect. 6). In this case the non-resonance condition is straightforwardly checked, e.g., with a one-off numerical evaluation of $\beta_{1,2}$ or via the approximation provided by (39).

6 Weak dissipation and invariant manifolds

According to the discussion of Sect. 5, the limit case of zero dissipation, studied also in [22], can be recovered by letting $\xi = 0$. It is immediate to check from Prop. 5.1 that such a limit implies that λ_j are purely imaginary, i.e., the origin degenerates into an elliptic equilibrium (also called center). However, one wonders if part of the structure of the elliptic case persists also for $\xi > 0$. A discussion about this issue is given next.

The argument relies on Prop. 5.1, which provides the quantitative tools in order to exploit the smallness of ξ for a substantial simplification of the structure of Eq. (33). More precisely, by choosing $\xi = O(\varepsilon)$ (weak dissipation), by (40) and (33) one finds that $I_j(\tau) = I_j(0) + O(\varepsilon^2)$, i.e., I_j approximates (in the perturbative sense) the first integrals of motion. As a consequence, in this setting, the invariant manifolds of the normalized system simply read as

$$\mathcal{M} := \mathcal{M}_1 \cup \mathcal{M}_2,$$
$$\mathcal{M}_j := \{I_j \equiv A_j \in (0, +\infty),\ \boldsymbol{\varphi} \in \mathbb{T}^2\}, \tag{42}$$

being A_j a real variable parameterizing the "flat" manifold $I_j = const.$ in the normalized system. A convenient (and often customary) way to visualize $\mathcal{M}$ is by plotting $\mathcal{M}_1$ and $\mathcal{M}_2$ separately.

A way to compute the first-order approximation of the invariant manifolds, in the nonnormalized system, is to map "back" the above-defined (flat) manifolds $\mathcal{M}_j$ via the variables transformation (26). The obtained objects are conveniently represented via the variables $\boldsymbol{\mathcal{I}}$, implicitly defined by the transformation $\mathcal{T}_{\boldsymbol{x}} : (\boldsymbol{\mathcal{I}}, \boldsymbol{\phi}) \to (\boldsymbol{x})$ given by

$$(x_{2j-1}, x_{2j}) = \sqrt{\mathcal{I}_j}\left(\exp(i\,\phi_j), \exp(-i\,\phi_j)\right), \tag{43}$$

for $j = 1, 2$. The set $(\boldsymbol{\mathcal{I}}, \boldsymbol{\phi})$ is easily interpreted as equivalent, under the weak dissipation assumption, to the set $(\boldsymbol{I}, \boldsymbol{\varphi})$ used in the normalized system. In fact, if $\xi = O(\varepsilon)$, from (38) one obtains that $\exp(\alpha_j \tau) = 1 + O(\varepsilon)$ for any $\tau = O(1)$. Hence, (43) is equivalent to the transformation $\mathcal{T}_{\boldsymbol{X}} : (\boldsymbol{I}, \boldsymbol{\varphi}) \to (\boldsymbol{X})$ obtained as the composition of (28), (31) and (32) where terms of order $O(\varepsilon)$ are disregarded. This implies that the invariant manifolds of the weak dissipation case possess exactly the same structure as the $\xi = 0$ limit. As a standard remark in classical perturbation theory, it is understood

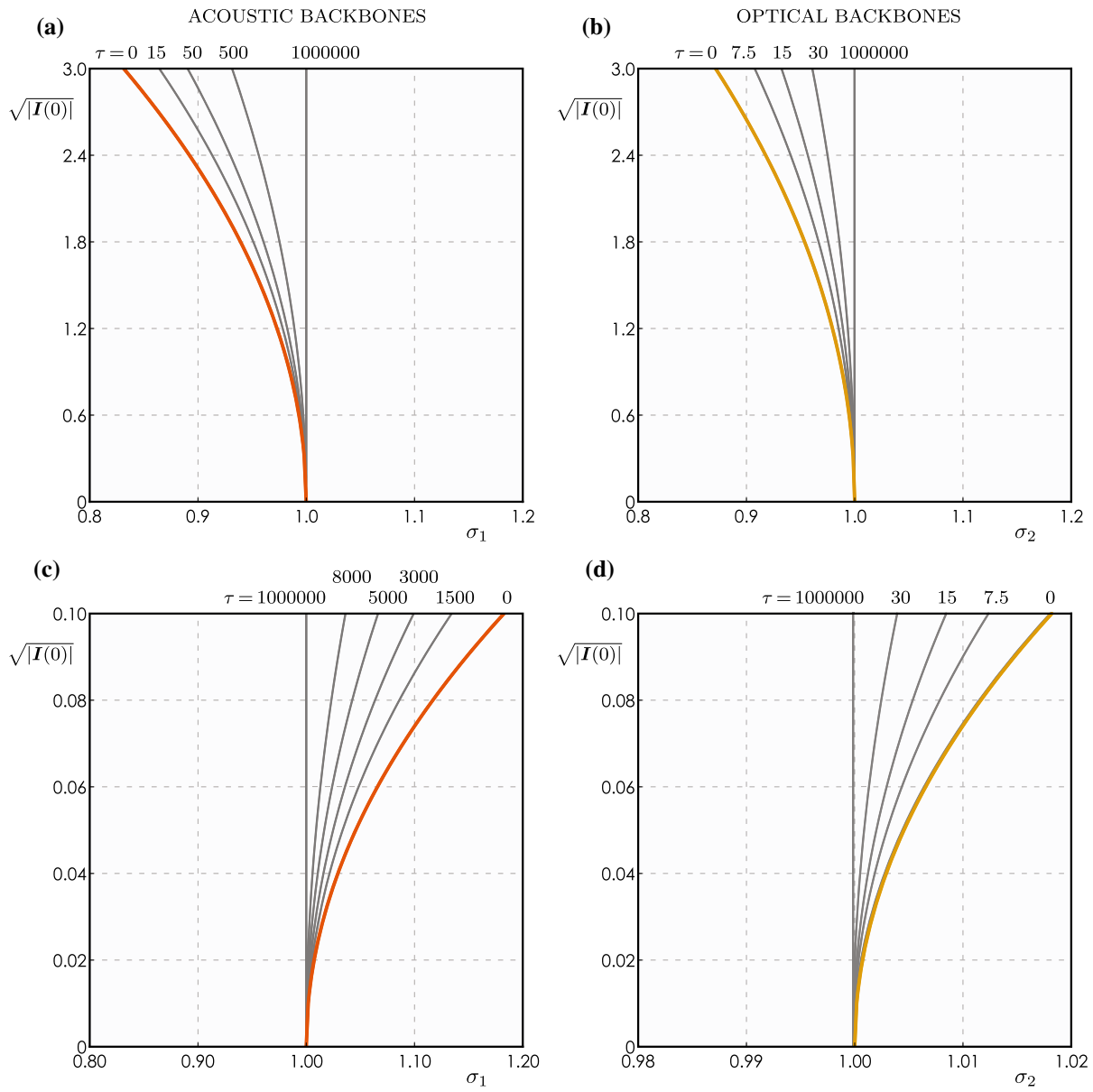

Fig. 6 Backbone curves σ_j versus squared initial action $|\boldsymbol{I}(0)|$ in the limit of short wavelengths $\beta = \pi$ for (a),(b) *heavy* metamaterial with properties $\mu = 1/2$, $\varrho = 48/10$, $\eta = 5/100$, exhibiting softening behavior; *light* metamaterial with properties $\mu = 5/100$, $\varrho = 15$, $\eta = 1/2$, exhibiting hardening behavior. Nonlinear backbones without dissipation (colored lines) and with dissipation for increasing time instants (gray lines): **a**, **c** acoustic branch, **b**.**d** optical branch. (Color figure online)

that such an equivalence holds as long as $\tau = O(1)$, i.e., $\tau \ll \varepsilon^{-1}$. More on this aspect is given in Sect. 7.

In conclusion, the first-order approximation of the invariant manifolds can be written as

$$\tilde{\mathcal{M}}_j := \left\{ \left(\mathcal{T}_{\boldsymbol{x}}^{-1} \circ \mathcal{N}_r \circ \mathcal{T}_{\boldsymbol{X}}(\boldsymbol{A}, \boldsymbol{\varphi}) \right) |_j, \quad \boldsymbol{\varphi} \in \mathbb{T}^2 \right\}.$$

Similarly, by denoting with $\mathcal{T}_{\boldsymbol{u}} : (u, w, \dot{u}, \dot{w}) \to (\boldsymbol{x})$ the sequence of variables transformations from the state-space of configurational variables $(u, w, \dot{u}, \dot{w})$ to the original modal coordinates $\boldsymbol{x}$, one can define

$$\hat{\mathcal{M}} := \left\{ \left(\mathcal{T}_{\boldsymbol{u}}^{-1} \circ \mathcal{N}_r \circ \mathcal{T}_{\boldsymbol{X}}(\boldsymbol{A}, \boldsymbol{\varphi}) \right), \quad \boldsymbol{\varphi} \in \mathbb{T}^2 \right\}.$$

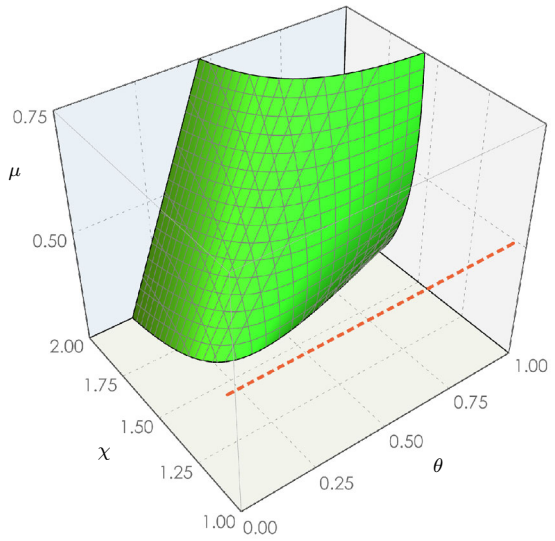

Fig. 7 Approximation of the resonant subset $\Pi_{1,2}(3)$ in the parameters space (θ, χ, μ) obtained by using Prop. 5.1 (green surface), and locus Γ of (θ, χ, μ)-parameters associated to the spectra reported in Fig. 4 (red dashed line) showing that the waves are sufficiently separated and away from the resonance conditions. (Color figure online)

This manifold can be conveniently visualized by projecting it on the two three-dimensional subspaces of configurational state variables $(u, \dot{u}, w)$ and $(w, \dot{w}, v)$, emphasizing the quasi-periodic nature of the motion.

A representation of the obtained manifolds is given in Figs. 8 and 9. Specifically, Fig. 8a illustrates the invariant manifold $\hat{\mathcal{M}}$ projected in the subsets of the state-space of the $(u, \dot{u}, w)$-variables while Fig. 8b shows the manifold projected in the space of the $(w, \dot{w}, u)$-variables. Differently, Fig. 9 portrays separately the invariant manifolds $\tilde{\mathcal{M}}_1$ and $\tilde{\mathcal{M}}_2$ in the sets of the $(\varphi_1, \varphi_2, \mathcal{I}_1)$-variables (Fig. 9a) and $(\varphi_1, \varphi_2, \mathcal{I}_2)$-variables (Fig. 9b), in which they are conveniently represented as open mono-valued surfaces.

7 Numerical validation

In this final section a validation example of the perturbation approach here employed is provided. The proposed procedure is straightforward: given an arbitrarily chosen point $\boldsymbol{p}$ on the invariant manifold, e.g., $\tilde{\mathcal{M}}_1$, the equations of motion (17) with $\xi = 0$ are integrated by using a fourth-order Runge-Kutta (RK4) scheme (see e.g., [81]) with $\boldsymbol{p}$ as initial condition. The resulting trajectory is superimposed in the plot of $\tilde{\mathcal{M}}_1$. By definition of $\tilde{\mathcal{M}}_{1,2}$, it is clear that the trajectory is expected to lie on the invariant surface for all $\tau \in [0, \tau^+]$, provided that τ^+ is not "too large". For instance, the numerical time integration reported in Fig. 10 is performed for $\tau^+ = 10$, whilst $\varepsilon^{-1} = 10^6$.

Remark 7.1 The real version of (17) has been used for numerical integration purposes as it avoids the machine treatment of complex numbers. More precisely, by using a transformation $\boldsymbol{x} = \boldsymbol{T}\,\boldsymbol{u}$ where $\boldsymbol{T}$ is the same matrix as the one defined in the right hand side of (28), system (17) is cast into the form

$$\begin{aligned} \dot{u}_{2j-1} &= \alpha_j u_{2j-1} - \beta_j u_{2j} + \sqrt{2}\varepsilon(\Re r_{2j-1})\tilde{\mathfrak{g}}\,(\boldsymbol{T}\,\boldsymbol{u})\,, \\ \dot{u}_{2j} &= \beta_j u_{2j-1} + \alpha_j u_{2j} + \sqrt{2}\varepsilon(\Re r_{2j-1})\tilde{\mathfrak{g}}\,(\boldsymbol{T}\,\boldsymbol{u})\,, \end{aligned} \tag{44}$$

for $j = 1, 2$. Note that variables u_j can be interpreted as the equivalent of U_j defined in (32).

As shown in Sect. 6 by means of perturbation tools, the system with a weak dissipation possesses the same first-order expansion of the invariant manifolds as the system in which the limit $\xi = 0$ is considered. The agreement between these manifolds and the trajectories (white curves) for the case $\xi = 0$ was proven in Fig. 10.

A completion of the numerical validation consists in showing that a similar agreement persists for trajectories for which $0 < \xi = O(\varepsilon)$ is considered. By denoting with $\boldsymbol{u}_\xi(\tau)$ the solutions of system (44) with a given initial condition $\boldsymbol{u}(0)$ and given dissipation ξ, the relative error is defined as

$$\mathcal{E}(\tau) := \frac{||\boldsymbol{u}_\xi(\tau) - \boldsymbol{u}_0(\tau)||}{\max_{\tau\in[0,\tau^+]} ||\boldsymbol{u}_0(\tau)||},$$

under the assumption that $\max_{\tau\in[0,\tau^+]} ||\boldsymbol{u}_0(\tau)||$ is bounded away from zero. The reference solution $\boldsymbol{u}_0(\tau)$ stands for the undamped solution ($\xi = 0$). Figure 11 shows the behavior of such a function, which is found to depend almost linearly on time, for increasing values of ξ. As expected, the error function grows proportionally to ξ. Specifically, a one-order-of-magnitude ξ-increment causes a like-order amplification of the error at a certain time instant.

8 Conclusions

A microstructured lattice waveguide, characterized by a diatomic periodic cell, was proposed as archety-

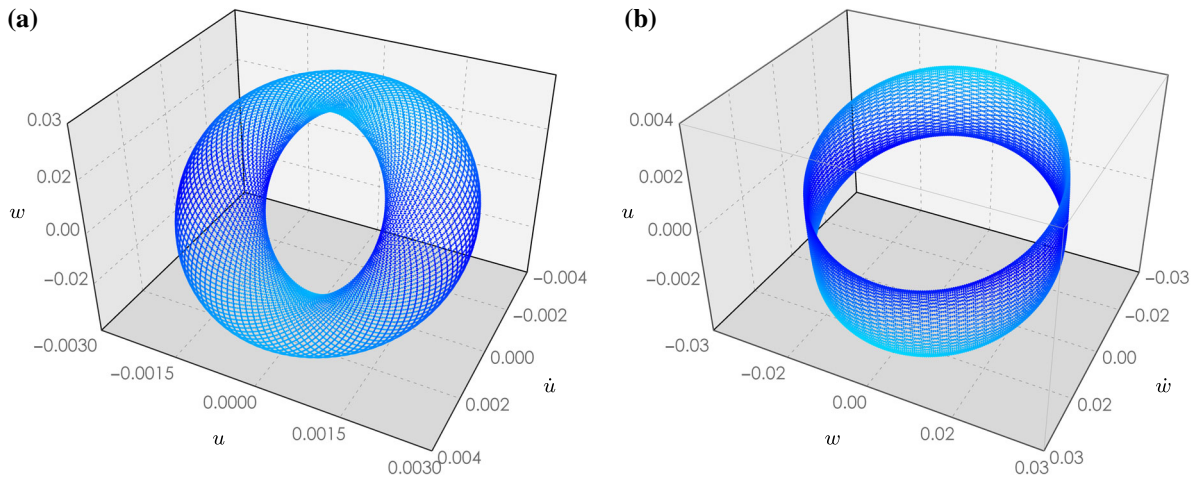

Fig. 8 Invariant manifold $\hat{\mathcal{M}}$ in the subset of configurational state variables: **a** subset $(u, \dot{u}, w)$-variables, **b** subset $(w, \dot{w}, u)$-variables

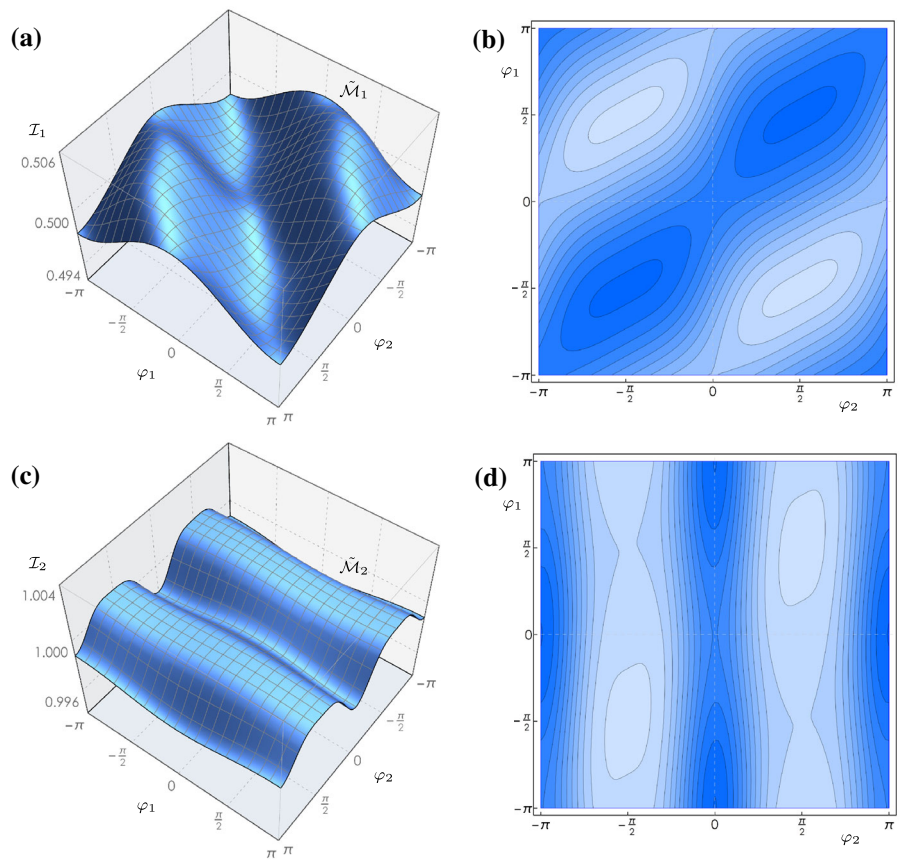

Fig. 9 Invariant surfaces where $(A_1, A_2) = (1/2, 1)$ have been chosen: **a**, **b** three-dimensional view and contour plot of the manifold $\tilde{\mathcal{M}}_1$; **c**, **d** three-dimensional view and contour plot of the manifold $\tilde{\mathcal{M}}_2$. The parameters are set as follows: $\mu = 1/40$, $\varrho^2 = 1/2$, $\eta = 1/2$, $\xi_1 = 0$, $\xi_2 = \xi_3 = 1/2$ and $\varepsilon = 10^{-6}$, i.e., solutions with $O(10^{-3})$ magnitude. In this particular case the frequencies $(\beta_1, \beta_2) = (0.5174, 0.9355)$ are away from $\mathfrak{R}$

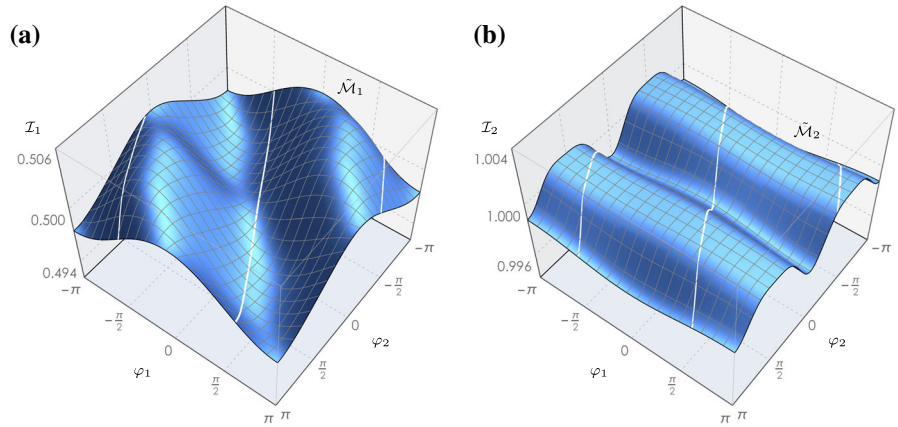

Fig. 10 The invariant surfaces $\tilde{\mathcal{M}}_{1,2}$ of Fig. 9 and the corresponding projections of the solution starting from $\boldsymbol{p}$. The parameters are the same as those employed in Fig. 9

pal physical realization of an acoustic locally dissipative metamaterial with highly tunable properties. A discrete Lagrangian two-degree-of-freedom model was formulated to govern the damped free dynamics of the periodic cell. The free propagation problem for the nonlinear waves through the dissipative lattice was formulated according to the Floquet-Bloch theory for periodic structures. In the framework of a finite kinematic formulation, the intracellular restoring forces are ruled by a nonlinear constitutive law, according to a parallel arrangement of nonlinear prestretched springs and a nonlinear dashpot, whereby the displacement and velocities of the principal atom and the secondary atom are coupled. The periodic cell was designed to act as a highly tunable vibration absorber featuring nonlinear hardening/softening response with nonlinear hysteretic dissipation.

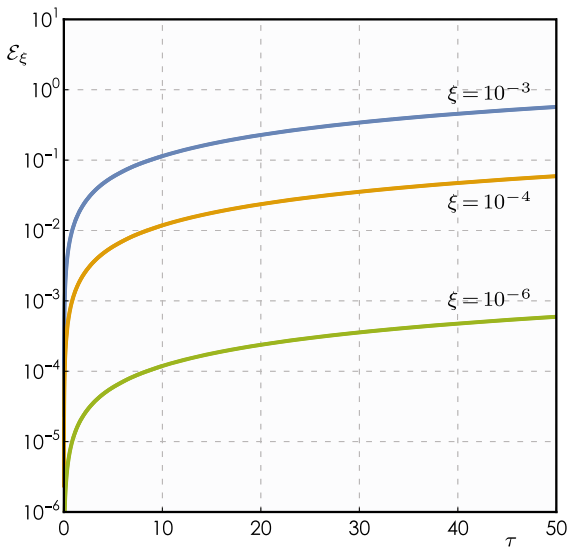

Fig. 11 Error function $\mathcal{E}_\xi$ (in logarithmic scale) versus time for $\mu = 1/40$, $\eta = 1/2$, $\varrho^2 = 1/2$, $\xi_2 = \xi_3 = 1/2$, $\varepsilon = 10^{-6}$ and different ξ-values

In order to study the dynamic regime of relatively high oscillation amplitudes, the nonlinear interatomic interaction was consistently approximated by retaining cubic terms in the intracellular stiffness and damping. A valuable functional customization is enabled by the high nonlinear tunability of the cell according to which the cubic stiffness can be designed to realize either a softening or a hardening behavior, by independently regulating the geometric (i.e., pretension) and elastic stiffness contributions of the intracellular springs.

The linear dispersion properties ensuing from the linearized eigenproblem governing the free wave propagation in the small-amplitude oscillation regime were summarized. The linear spectrum is composed by a low-frequency acoustic branch and a high-frequency optical branch, described by complex-valued dispersion functions. A perturbation expression of the negative real part (ruling the wave attenuation) and imaginary part (ruling the wave frequency) of the dispersion function was achieved, assuming the weak damping coefficient as small parameter. The parametric conditions of 2:1, 1:1 and 3:1 autoparametric resonances between the waves associated with the acoustic and the optical branches were determined analytically so as to study asymptotically the nonlinear waves propagating as distinct, individual acoustic or optical waves away from internal coupling conditions.

The nonlinear dispersion properties were unfolded by employing an extended Hamiltonian perturbation technique accounting also for the nonlinear dissipa-

tion. By restricting the attention onto internally non-resonant metamaterial lattices, a perturbation scheme based on Lie series operators was devised to asymptotically approximate the free wave motion up to the lowest significant perturbation order. The nonlinear dispersion properties were obtained as analytical time-dependent functions, depending linearly on the initial values of a suitable pair of variables (action-angle).

An original contribution is that the nonlinear wave frequencies were found to (i) exhibit softening or hardening backbone curves for increasing amplitudes depending on the cubic stiffness coefficient of the intracellular spring, and (ii) consistently tend to coalesce toward the linear spectrum of undamped, conservative metamaterials, for sufficiently long oscillation times when the decaying effects of the dissipation are such that the wave amplitudes become effectively small. Furthermore, the lowest-order approximation of the invariant manifolds, describing the harmonic periodic motions in the limit case of weak dissipation, were also analytically determined. An excellent agreement was systematically obtained from the direct comparison between the invariant manifolds predicted by the asymptotic results and the orbits described by numerical simulations.

The main findings of this work highlight the possibility of tailoring the metamaterial lattice properties to make the nonlinear waves faster (hardening case) or slower (softening case) and of making these nonlinear effects more or less persistent over time depending on the level of dissipation. Nonlinear hysteretic dissipation has far deeper effects on the nonlinear dynamics of engineered architectured waveguides which will be the focus of future works.

Acknowledgements This research was partially supported by the Italian Ministry of Education, University and Scientific Research under PRIN Grant No. 2017L7X3CS and by the Air Force Office of Scientific Research, Grant N. FA 8655-20-1-7025. The authors gratefully acknowledge the financial support from National Group of Mathematical Physics (GNFM-INdAM), from the Compagnia San Paolo, project MINIERA no. I34I20000380007 and from University of Trento, project UNMASKED 2020.

Data availability statement Relevant data can be made available upon request.

Declarations

Conflict of interest The authors declare no conflict of interest.

A Appendix

A.1 Proof of Proposition 2.1

Let $P_\lambda(\boldsymbol{A})$ denote the characteristic polynomial of $\boldsymbol{A}$ expressed as

$$\begin{aligned} P_\lambda(\boldsymbol{A}) &= \lambda^4 + \xi\chi\lambda^3 + 2p\lambda^2 + 2(\chi-1)\xi\theta\lambda + q \\ &= \lambda^2\left[\lambda^2 + \xi\chi\lambda + p\right] \\ &\quad + \left[p\lambda^2 + 2(\chi-1)\xi\theta\lambda + q\right], \end{aligned} \tag{45}$$

where $p := \mu\chi + \theta$ and $q := 4(\chi-1)\mu\theta$, respectively.

A sufficient condition for the statement to be true is that the two polynomials between square brackets do not possess real roots. This happens if either $\xi^2\chi^2 < 4p$ or $(\chi-1)\xi^2\theta < 4\mu p$, respectively. It is immediate to check that both of them hold under condition (13).

The property $\alpha_{1,2} < 0$ follows from the celebrated Routh-Hurwitz Theorem [82]. More precisely, from (45) it is possible to define

$$\mathfrak{M} := \{\mathfrak{m}_{i,j}\} = \begin{pmatrix} \xi\chi & 1 & 0 & 0 \\ 2(\chi-1)\xi\theta & 2p & \xi\chi & 1 \\ 0 & q & 2(\chi-1)\xi\theta & 2p \\ 0 & 0 & 0 & q \end{pmatrix},$$

and the quantities $\Delta_k := \det\left(\mathfrak{M}^{(\leq k)}\right)$, where $\mathfrak{M}^{(\leq k)} := \{\mathfrak{m}_{i,j}\}_{i,j\leq k}$ is the square submatrix of $\mathfrak{M}$ formed by the first k rows and columns. The property $\Re\lambda_j < 0$ for $\xi > 0$ easily follows from the mentioned Theorem, by observing that either $\Delta_1 \equiv \xi\chi$, or

$$\Delta_2 = 2\xi(\mu\chi^2 + \theta),\ \Delta_3 = 4\theta^2\xi^2(\chi-1),$$
$$\Delta_4 = 16\mu\theta^3\xi^2(\chi-1)^2,$$

are positive by assumptions on the parameters.

Finally, the property $\beta_{1,2} > 0$ is easily shown by *reductio ad absurdum*. For this purpose, it is worth recalling that the eigenvalues are non-purely real, as previously shown. On the other hand, Prop. 5.1 states that for any $\tilde{\boldsymbol{\zeta}} := (\tilde{\xi}, \tilde{\varrho}, \tilde{\mu}, \tilde{\theta})$ satisfying Eq. (36) and sufficiently small ξ, it turns out that $\beta_{1,2} = \beta_{1,2}(\tilde{\boldsymbol{\zeta}}) > 0$. Next, suppose by contradiction, that for some other value $\hat{\boldsymbol{\zeta}}$ (under the sole assumption (13)), one has $\beta_1(\hat{\boldsymbol{\zeta}}) < 0$ (the argument for β_2 is the same). Hence, once defined, for all $j = 1, ..., 4$, $\zeta_j(s_j) := s_j\tilde{\zeta}_j + (1-s_j)\hat{\zeta}_j$, with $\boldsymbol{s} \in [0,1]^4$, there exists $\boldsymbol{s}^*$ such that $\beta_1(\boldsymbol{\zeta}(\boldsymbol{s}^*)) = 0$, i.e., $\lambda_1 \in \mathbb{R}$, which is a contradiction.

A.2 Proof of Prop 5.1

The stated range of variation of Θ follows directly from (36) and the fact that $\chi > 1$ by definition. By assumption, the characteristic polynomial $P_\lambda(\boldsymbol{A})$ is factorized as

$$P_\lambda(\boldsymbol{A}) = \prod_{j=1}^{4}(\lambda - \lambda_j), \tag{46}$$

with $\lambda_{2k-1} = \bar{\lambda}_{2k}$, $k = 1, 2$. By using the expansions (37) in (14), then substituting back into (46) and finally comparing the obtained expression with (45), one gets at zero order in ξ

$$b_1 + b_2 = 2(\mu\chi + \theta), \tag{47}$$
$$b_1 b_2 = 4\theta\mu(\chi - 1), \tag{48}$$

which give (39). On the other hand, at first order in ξ, the following set of conditions is obtained:

$$b_2 a_1 + b_1 a_2 = (\chi - 1)\theta, \tag{49}$$
$$2(a_1 + a_2) = \chi, \tag{50}$$

leading to (38).

Focusing first on the non-resonance property, it is clear from (16) that

$$\boldsymbol{\Psi} = \boldsymbol{\Psi}_0 + O(\xi),$$
$$\boldsymbol{\Psi}_0 := \boldsymbol{\Psi}|_{(\lambda_1,\lambda_2,\lambda_3,\lambda_4)=(\beta_1,\beta_1,\beta_2,\beta_2)}. \tag{51}$$

In particular, the third row entries of $\boldsymbol{\Psi}_0$ are pure real at order zero in ξ. Hence, as $\xi_1 = O(\xi)$ by definition, a comparison between (12) and (23) yields

$$\Im\gamma_{\boldsymbol{\nu}} = O(\xi). \tag{52}$$

Moreover, from (51), it is easy to check that

$$\det(\boldsymbol{\Psi}_0) = 16(\beta_1\beta_2)^{-3}(\beta_2 - \beta_1)^2 \times(\beta_1 + \beta_2)^2(\chi - 1)\theta^2,$$

i.e., $\boldsymbol{\Psi}_0$ is invertible away from $\mathfrak{R}$, so is $\boldsymbol{\Psi}$, for sufficiently small ξ. In particular, the fourth column of $\boldsymbol{\Psi}_0^{-1}$ yields

$$r_{1,2} = \mp i[2(b_1 - b_2)]^{-1}\sqrt{b_1} + O(\xi),$$
$$r_{3,4} = \pm i[2(b_1 - b_2)]^{-1}\sqrt{b_2} + O(\xi),$$

where the expression in terms of the parameters is obtained from (39). The latter implies $\Re r_j = O(\xi)$, which compared with (52) gives (40).

Focusing finally on Eq. (41), it can be observed that $\lim_{(\xi,\theta)\to(0,0)^+}(\beta_1, \beta_2) = (0, 2\sqrt{\mu\chi})$. Hence, by continuity, for any sufficiently small ξ and θ, the curve $(\beta_1(\theta), \beta_2(\theta))$ "starts" inside the region

$$\mathfrak{T} := \{\beta_2 > 3\beta_1,\ \beta_1 > 0\} \subset \mathbb{R}^2.$$

The statement easily follows for sufficiently small ξ by using (39). In fact, it is easy to check that, under assumption (36), one has $b_2 > 9b_1$ for all $\theta \in (0, 1)$.

A.3 Expression of the coefficients $\gamma_{\boldsymbol{\nu}}$

Recalling that $\zeta := \xi_1\xi_2\xi_3$ and $\kappa := \mu - \eta$ and denoting by Ψ_{ij} the elements of matrix $\boldsymbol{\Psi}$, the coefficients $\gamma_{\boldsymbol{\nu}}$ read

$$\begin{aligned}
\gamma_{(3,0,0,0)} &= \Psi_{21}^3\kappa - \zeta\Psi_{21}^2\Psi_{41}\chi + \zeta\Psi_{21}^2\Psi_{31}^2\\
\gamma_{(0,3,0,0)} &= \Psi_{22}^3\kappa - \zeta\Psi_{22}^2\Psi_{42}\chi + \zeta\Psi_{22}^2\Psi_{32}^2\\
\gamma_{(0,0,3,0)} &= \Psi_{23}^3\kappa + \zeta\Psi_{23}^3(\Psi_{33} - \chi\Psi_{43})\\
\gamma_{(0,0,0,3)} &= \Psi_{24}^3\kappa + \zeta\Psi_{24}^2(\Psi_{34} - \Psi_{44}\chi)\\
\gamma_{(1,1,1,0)} &= 6\Psi_{21}\Psi_{22}\Psi_{23}\kappa\\
&\quad - 2\zeta\chi(\Psi_{21}\Psi_{22}\Psi_{43} - \Psi_{21}\Psi_{23}\Psi_{42} - \Psi_{22}\Psi_{23}\Psi_{41})\\
&\quad + 2\zeta(\Psi_{21}\Psi_{22}, \Psi_{33} + \Psi_{21}\Psi_{23}\Psi_{32} + \Psi_{22}\Psi_{23}\Psi_{31})\\
\gamma_{(1,0,1,1)} &= 6\Psi_{21}\Psi_{23}\Psi_{24}\kappa\\
&\quad - 2\zeta\chi(\Psi_{21}\Psi_{23}\Psi_{44} - \Psi_{21}\Psi_{24}\Psi_{43} - \Psi_{23}\Psi_{24}\Psi_{41})\\
&\quad + 2\zeta(\Psi_{21}\Psi_{23}\Psi_{34} + \Psi_{21}\Psi_{24}\Psi_{33} + \Psi_{23}\Psi_{24}\Psi_{31})\\
\gamma_{(0,1,1,1)} &= 6\Psi_{22}\Psi_{23}\Psi_{24}\kappa\\
&\quad - 2\zeta\chi(\Psi_{22}\Psi_{23}\Psi_{44} - \Psi_{22}\Psi_{24}\Psi_{43} - \Psi_{23}\Psi_{24}\Psi_{42})\\
&\quad + 2\zeta(\Psi_{22}\Psi_{23}\Psi_{34} + \Psi_{22}\Psi_{24}\Psi_{33} + \Psi_{23}\Psi_{24}\Psi_{32})\\
\gamma_{(0,0,1,2)} &= 3\Psi_{23}\Psi_{24}^2\kappa - \zeta\chi(\Psi_{24}^2\Psi_{43} - 2\Psi_{23}\Psi_{24}\Psi_{44})\\
&\quad + \zeta(\Psi_{24}^2\Psi_{33} + 2\Psi_{23}\Psi_{24}\Psi_{34})\\
\gamma_{(0,1,0,2)} &= 3\Psi_{22}\Psi_{24}^2\kappa - \zeta\chi(\Psi_{24}^2\Psi_{42} - 2\Psi_{22}\Psi_{24}\Psi_{44})\\
&\quad + \zeta(\Psi_{24}^2\Psi_{32} + 2\Psi_{22}\Psi_{24}\Psi_{34})\\
\gamma_{(1,0,0,2)} &= 3\Psi_{21}\Psi_{24}^2\kappa - \zeta\chi(\Psi_{24}^2\Psi_{41} - 2\Psi_{21}\Psi_{24}\Psi_{44})\\
&\quad + \zeta(\Psi_{24}^2\Psi_{31} + 2\Psi_{21}\Psi_{24}\Psi_{34})\\
\gamma_{(0,0,2,1)} &= 3\Psi_{23}^2\Psi_{24}\kappa - \zeta\chi(\Psi_{23}^2\Psi_{44} - 2\Psi_{23}\Psi_{24}\Psi_{43})\\
&\quad + \zeta(\Psi_{22}^2\Psi_{34} + 2\Psi_{22}\Psi_{24}\Psi_{32})\\
\gamma_{(2,0,1,0)} &= 3\Psi_{21}^2\Psi_{23}\kappa - \zeta\chi(\Psi_{21}^2\Psi_{43} - 2\Psi_{21}\Psi_{23}\Psi_{41})\\
\gamma_{(2,0,0,1)} &= 3\Psi_{21}^2\Psi_{24}\kappa - \zeta\chi(\Psi_{21}^2\Psi_{44} - 2\Psi_{22}\Psi_{24}\Psi_{42})\\
&\quad + \zeta(\Psi_{22}^2\Psi_{34} + 2\Psi_{22}\Psi_{24}\Psi_{32})\\
\gamma_{(0,1,2,0)} &= 3\Psi_{22}\Psi_{23}^2\kappa - \zeta\chi(\Psi_{23}^2\Psi_{42} - 2\Psi_{22}\Psi_{23}\Psi_{43})\\
&\quad + \zeta(\Psi_{23}^2\Psi_{32} + 2\Psi_{22}\Psi_{23}\Psi_{33})
\end{aligned}$$

$$\gamma_{(1,0,2,0)} = 3\Psi_{21}\Psi_{23}^2\kappa - \zeta\chi(\Psi_{23}^2\Psi_{41} - 2\Psi_{21}\Psi_{23}\Psi_{43}) + \zeta(\Psi_{23}^2\Psi_{31} + 2\Psi_{21}\Psi_{23}\Psi_{33})$$

$$\gamma_{(0,2,1,0)} = 3\Psi_{22}^2\Psi_{23}\kappa - \zeta\chi(\Psi_{22}^2\Psi_{43} - 2\Psi_{22}\Psi_{23}\Psi_{42}) + \zeta(\Psi_{22}^2\Psi_{33} + 2\Psi_{22}\Psi_{23}\Psi_{32})$$

$$\gamma_{(2,0,1,0)} = 3\Psi_{21}^2\Psi_{23}\kappa - \zeta\chi(\Psi_{21}^2\Psi_{43} - 2\Psi_{21}\Psi_{23}\Psi_{41}) + \zeta(\Psi_{21}^2\Psi_{33} + 2\Psi_{21}\Psi_{23}\Psi_{31})$$

$$\gamma_{(1,2,0,0)} = 3\Psi_{21}\Psi_{22}^2\kappa - \zeta\chi(\Psi_{22}^2\Psi_{41} - 2\Psi_{21}\Psi_{22}\Psi_{42}) + \zeta(\Psi_{22}^2\Psi_{31} + 2\Psi_{21}\Psi_{22}\Psi_{32})$$

$$\gamma_{(2,1,0,0)} = 3\Psi_{21}^2\Psi_{22}\kappa - \zeta\chi(\Psi_{21}^2\Psi_{42} - 2\Psi_{21}\Psi_{22}\Psi_{41}) + \zeta(\Psi_{21}^2\Psi_{32} + 2\Psi_{21}\Psi_{22}\Psi_{31})$$

Remark A.1 It can be noted that ζ vanishes in the "zero dissipation limit" $\xi_1 = 0$.

References

1. Hussein, M.I., Frazie, M.J.: Metadamping: an emergent phenomenon in dissipative metamaterials. J. Sound Vib. **332**(20), 4767–4774 (2013)
2. Friedrich, K., Breuer, U.: Multifunctionality of Polymer Composites: Challenges and New Solutions. Elsevier, Amsterdam (2015)
3. Ferreira, A.D.B., Nóvoa, P.R., Marques, A.T.: Multifunctional material systems: a state-of-the-art review. Compos. Struct. **151**, 3–35 (2016)
4. Lincoln, R.L., Scarpa, F., Ting, V.P., et al.: Multifunctional composites: a metamaterial perspective. Multifunct. Mater. **2**(4), 043001 (2019)
5. Arena, A., Taló, M., Snyder, M.P., et al.: Enhancing flutter stability in nanocomposite thin panels by harnessing CNT/polymer dissipation. Mech. Res. Commun. **104**, 103495 (2020)
6. Arena, A., Lacarbonara, W.: Piezoelectrically induced nonlinear resonances for dynamic morphing of lightweight panels. J. Sound Vib. **498**, 115951 (2021)
7. Talò, M., Lanzara, G., Krause, B., et al.: "Sliding Crystals" on low-dimensional carbonaceous nanofillers as distributed nanopistons for highly damping materials. ACS Appl. Mater. Interfaces **11**(41), 38147–38159 (2019)
8. Formica, G., Lacarbonara, W.: Asymptotic dynamic modeling and response of hysteretic nanostructured beams. Nonlinear Dyn. **99**, 227–248 (2020)
9. Schaedler, T.A., Carter, W.B.: Architected cellular materials. Ann. Rev. Mater. Res. **46**, 187–210 (2016)
10. Kadic, M., Milton, G.W., van Hecke, M., et al.: 3D metamaterials. Nat. Rev. Phys. **1**, 198–210 (2019)
11. Wang, Y.-F., Wang, Y.-Z., Wu, B., et al.: Tunable and active phononic crystals and metamaterials. Appl. Mech. Rev. **72**(4), 040801 (2020)
12. Cummer, S.A., Christensen, J., Alù, A.: Controlling sound with acoustic metamaterials. Nat. Rev. Mater. **1**(3), 1–13 (2016)
13. Bacigalupo, A., Lepidi, M.: Acoustic wave polarization and energy flow in periodic beam lattice materials. Int. J. Solids Struct. **147**, 183–203 (2018)
14. D'Alessandro, L., Ardito, R., Braghin, F., et al.: Low frequency 3D ultra-wide vibration attenuation via elastic metamaterial. Sci. Rep. **9**(1), 1–8 (2019)
15. Dal Corso, F., Tallarico, D., Movchan, N.V., et al.: Nested Bloch waves in elastic structures with configurational forces. Philos. Trans. R. Soc. A **377**(2156), 20190101 (2019)
16. Fang, L., Darabi, A., Mojahed, A., et al.: Broadband nonreciprocity with robust signal integrity in a triangle-shaped nonlinear 1D metamaterial. Nonlinear Dyn. **100**, 1–13 (2020)
17. Meng, H., Huang, X., Chen, Y., et al.: Structural vibration absorption in multilayered sandwich structures using negative stiffness nonlinear oscillators. Appl. Acoust. **182**, 108240 (2021)
18. Zhu, H.-P., Chen, H.-Y.: Parameter modulation of periodic waves and solitons in metamaterials with higher-order dispersive and nonlinear effects. Nonlinear Dyn. **104**(2), 1545–1554 (2021)
19. Wang, C., Kanj, A., Mojahed, A., et al.: Wave redirection, localization, and non-reciprocity in a dissipative nonlinear lattice by macroscopic Landau-Zener tunneling: Theoretical results. J. Appl. Phys. **129**(9), 095105 (2021)
20. Askari, M., Hutchins, D.A., Thomas, P.J., et al.: Additive manufacturing of metamaterials: a review. Addit. Manuf. **36**, 101562 (2020)
21. Deymier, P.A.: Acoustic Metamaterials and Phononic Crystals, Volume 173 of Springer Series in Solid-State Sciences. Springer-Verlag, Berlin Heidelberg (2013)
22. Lepidi, M., Bacigalupo, A.: Wave propagation propertiesof one-dimensional acoustic metamaterials with nonlinear diatomic microstructure. Nonlinear Dyn. **98**(4), 2711–2735 (2019)
23. Vadalà, F., Bacigalupo, A., Lepidi, M., et al.: Free and forced wave propagation in beam lattice metamaterials with viscoelastic resonators. Int. J. Mech. Sci. **193**, 106129 (2021)
24. Bacigalupo, A., Gambarotta, L.: Dispersive wave propagation in two-dimensional rigid periodic blocky materials with elastic interfaces. J. Mech. Phys. Solids **102**, 165–186 (2017)
25. Beli, D., Arruda, J.R.F., Ruzzene, M.: Wave propagationin elastic metamaterial beams and plates with interconnected resonators. Int. J. Solids Struct. **139**, 105–120 (2018)
26. Deng, B., Wang, P., He, Q., et al.: Metamaterials with amplitude gaps for elastic solitons. Nat. Commun. **9**, 1–9 (2018)
27. Carboni, B., Lacarbonara, W.: Nonlinear dynamic response of a new hysteretic rheological device: experiments and computations. Nonlinear Dyn. **83**, 23–39 (2016)
28. Casalotti, A., Lacarbonara, W.: Tailoring of pinched hysteresis for nonlinear vibration absorption via asymptotic analysis. Int. J. Non-Linear Mech. **94**, 59–71 (2017)
29. Casalotti, A., El-Borgi, S., Lacarbonara, W.: Metamaterial beam with embedded nonlinear vibration absorbers. Int. J. Non-Linear Mech. **98**, 32–42 (2018)
30. Muhammad, Lim, C.W., Li, J.T.H., et al.: Lightweight architected lattice phononic crystals with broadband and multiband vibration mitigation characteristics. Extreme Mech. Lett. **41**, 100994 (2020)

31. Wu, L., Geng, Q., Li, Y.-M.: A locally resonant elastic metamaterial based on coupled vibration of internal liquid and coating layer. J. Sound Vib. **468**, 115102 (2020)
32. Manimala, J.M., Sun, C.: Microstructural design studies for locally dissipative acoustic metamaterials. J. Appl. Phys. **115**(2), 023518 (2014)
33. Bacigalupo, A., Gnecco, G., Lepidi, M., et al.: Computational design of innovative mechanical metafilters via adaptive surrogate-based optimization. Comput. Methods Appl. Mech. Eng. **375**, 113623 (2021)
34. Lepidi, M., Bacigalupo, A.: Multi-parametric sensitivity analysis of the band structure for tetrachiral acoustic metamaterials. Int. J. Solids Struct. **136–137**, 186–202 (2018)
35. Kochmann, D.M., Hopkins, J.B., Valdevit, L.: Multiscale modeling and optimization of the mechanics of hierarchical metamaterials. MRS Bull. **44**, 773–781 (2019)
36. Zhou, J., Dou, L., Wang, K., et al.: A nonlinear resonator with inertial amplification for very low-frequency flexural wave attenuations in beams. Nonlinear Dyn. **96**, 647–665 (2019)
37. Lepidi, M., Bacigalupo, A.: Nonlinear dispersion properties of acoustic waveguides with cubic local resonators. In: Developments and Novel Approaches in Biomechanics and Metamaterials, pp. 377–392. Springer, New York (2020)
38. Bukhari, M., Barry, O.: Spectro-spatial analyses of a nonlinear metamaterial with multiple nonlinear local resonators. Nonlinear Dyn. **99**, 1539–1560 (2020)
39. Xu, L., Rahmani, M., Powell, D.A., et al.: Nonlinear Metamaterials, pp. 55–79. Springer International Publishing, Cham (2020)
40. Nayfeh, A.H., Mook, D.T.: Nonlinear oscillations. Wiley, New York, US (2008)
41. Fronk, M.D., Leamy, M.J.: Internally resonant wave energy exchange in weakly nonlinear lattices and metamaterials. Phys. Rev. E **100**, 032213 (2019)
42. Settimi, V., Lepidi, M., Bacigalupo, A.: Nonlinear dispersion properties of one-dimensional mechanical metamaterials with inertia amplification. Int. J. Mech. Sci. **201**, 106461 (2021)
43. Vakakis, A.F., King, M.E.: Nonlinear wave transmission in a monocoupled elastic periodic system. J. Acoust. Soc. Am. **98**(3), 1534–1546 (1995)
44. Vakakis, A.F., King, M.E.: Resonant oscillations of a weaklycoupled, nonlinear layered system. Acta Mech. **128**(1–2), 59–80 (1998)
45. Manktelow, K., Leamy, M.J., Ruzzene, M.: Multiple scales analysis of wave-wave interactions in a cubically nonlinear monoatomic chain. Nonlinear Dyn. **63**, 193–203 (2011)
46. Silva, P.B., Leamy, M.J., Geers, M.G.D., et al.: Emergent subharmonic band gaps in nonlinear locally resonant metamaterials induced by autoparametric resonance. Phys. Rev. E **99**(6), 063003 (2019)
47. Wattis, J.A.D.: Quasi-continuum approximations to lattice equations arising from the discrete nonlinear telegraph equation. J. Phys. A Math. Gen. **33**(33), 5925 (2000)
48. Bacigalupo, A., Gambarotta, L.: Generalized micropolar continualization of 1D beam lattices. Int. J. Mech. Sci. **155**, 554–570 (2019)
49. Bacigalupo, A., Gambarotta, L., Lepidi, M.: Thermodynamically consistent non-local continualization for masonry-like systems. Int. J. Mech. Sci. **205**, 106538 (2021)
50. Porubov, A.: Wave modulation in a nonlinear acoustic metamaterial. Int. J. Non-Linear Mech. **137**, 103788 (2021)
51. Mojahed, A., Vakakis, A.F.: Certain aspects of the acoustics of a strongly nonlinear discrete lattice. Nonlinear Dyn. **99**, 643–659 (2020)
52. Romeo, F., Rega, G.: Propagation properties of bi-coupled nonlinear oscillatory chains: analytical prediction and numerical validation. Int. J. Bifurc. Chaos **18**(7), 1983–1998 (2008)
53. Lazarov, B.S., Jensen, J.S.: Low-frequency band gaps inchains with attached non-linear oscillators. Int. J. Non-Linear Mech. **42**(10), 1186–1193 (2007)
54. Sridhar, A., Kouznetsova, V.G., Geers, M.G.D.: A general multiscale framework for the emergent effective elastodynamics of metamaterials. J. Mech. Phys. Solids **111**, 414–433 (2018)
55. Narisetti, R.K., Leamy, M.J., Ruzzene, M.: A perturbation approach for predicting wave propagation in one-dimensional nonlinear periodic structures. J. Vib. Acoust. **132**(3), 031001 (2010)
56. Narisetti, R., Ruzzene, M., Leamy, M.J.: A perturbation approach for analyzing dispersion and group velocities in two-dimensional nonlinear periodic lattices. J. Vib. Acoust. **133**(6), 061020 (2011)
57. Fang, X., Wen, J., Yin, J., et al.: Wave propagation in nonlinear metamaterial multi-atomic chains based on homotopy method. AIP Adv. **6**(12), 121706 (2016)
58. Fang, X., Wen, J., Yin, J., et al.: Broadband and tunable one-dimensional strongly nonlinear acoustic metamaterials: theoretical study. Phys. Rev. E **94**(5), 052206 (2016)
59. Fortunati, A., Wiggins, S.: Integrability and strong normal forms for non-autonomous systems in a neighbourhood of an equilibrium. J. Math. Phys. **57**(9), 092703 (2016)
60. Fortunati, A., Wiggins, S.: A Lie transform approach to the construction of Lyapunov functions in autonomous and non-autonomous systems. J. Math. Phys. **60**(8), 082704 (2019)
61. Poincaré, H.: Les Méthodes Nouvelles de la Mécanique Céleste. Gauthier-Villars, Paris (1892)
62. Eliasson, L.H.: Absolutely convergent series expansions for quasi periodic motions. Math. Phys. Electron. J. **2**(4), 33 (1996)
63. Gallavotti, G.: Twistless KAM tori, quasi flat homoclinic intersections, and other cancellations in the perturbation series of certain completely integrable Hamiltonian systems: a review (1994)
64. Chierchia, L., Falcolini, C.: A direct proof of a theorem by Kolmogorov in Hamiltonian systems. Ann. Sc. Norm. Sup. Pisa Cl. Sci. **21**, 541–593 (1994)
65. Nekhoroshev, N.N.: An exponential estimate on the time of stabilty of nearly-integrable Hamiltonian systems. Russ. Math. Surv. **32**, 1–65 (1977)
66. Nekhoroshev, N.N.: An exponential estimate on the time of stabilty of nearly-integrable Hamiltonian systems II. Trudy Sem. Petrovsk. **5**, 5–50 (1979)
67. Chierchia, L.: Kolmogorov-Arnold-Moser (KAM) Theory. (2009)
68. Giorgilli, A., Galgani, L.: Formal integrals for an autonomous Hamiltonian system near an equilibrium point. Celest. Mech. **17**, 267–280 (1978)
69. Ferraz-Mello, S.: Lie Series Perturbation Theory, pp. 139–159. Springer, New York, New York, NY (2007)

70. Giorgilli, A.: Notes on exponential stability of Hamiltonian systems. Centro di Ricerca Matematica Ennio De Giorgi, Pisa, Italy (2002)
71. Giorgilli, A., Zehnder, E.: Exponential stability for time dependent potentials. Z. Angew. Math. Phys. (ZAMP) **43**, 827–855 (1992)
72. Fortunati, A., Wiggins, S.: Normal forms à la Moser for aperiodically time-dependent Hamiltonians in the vicinity of a hyperbolic equilibrium. Discrete Contin. Dyn. Syst. Ser. S **9**(4), 1109–1118 (2016)
73. Fortunati, A., Wiggins, S.: Negligibility of small divisor effects in the normal form theory for nearly-integrable Hamiltonians with decaying non-autonomous perturbations. Celest. Mech. Dyn. Astron. **125**(2), 247–262 (2016)
74. Carboni, B., Arena, A., Lacarbonara, W.: Nonlinear vibration absorbers for ropeway roller batteries control. In: Proceedings of the Institution of Mechanical Engineers, Part C: Journal of Mechanical Engineering Science, p. 0954406220953454 (2020)
75. Brillouin, L.: Wave Propagation and Group Velocity, vol. 8. Academic press, Cambridge (2013)
76. Giorgilli, A.: On the representation of maps by Lie trasforms. Rendiconti dell'Istituto Lombardo Accademia di Scienze e Lettere, Classe di Scienze 251–277 (2012)
77. Berdichevsky, V.: Variational principles of continuum mechanics. I: fundamentals. In: Interaction of Mechanics and Mathematics. Springer, Berlin Heidelberg (2009)
78. Shilnikov, L.P.: Methods of Qualitative theory in nonlinear dynamics. In: Number v. 1 in Methods of Qualitative Theory in Nonlinear Dynamics. World Scientific, Singapore (1998)
79. Nayfeh, A.H., Mook, D.T.: Parametric excitations of linear systems having many degrees of freedom. J. Acoust. Soc. Am. **62**(2), 375–381 (1977)
80. Eslami, H., Kandil, O.A.: Nonlinear forced vibration of orthotropic rectangular plates using the method of multiple scales. AIAA J. **27**(7), 955–960 (1989)
81. Quarteroni, A., Sacco, R., Saleri, F.: Numerical Mathematics. Texts in Applied Mathematics. Springer, New York (2017)
82. Gradshteyn, I., Ryzhik, I.: Table of Integrals, Series, and Products. Elsevier Science, Amsterdam (2014)